

Article

Development of anilino-maytansinoid ADCs that efficiently release cytotoxic metabolites in cancer cells and induce high levels of bystander killing

Wayne C. Widdison, Jose F Ponte, Jennifer A Coccia, Leanne Lanieri, Yulius Setiady, Ling Dong, Anna Skaletskaya, E. Erica Hong, Rui Wu, Qifeng Qiu, Rajeeva Singh, Paulin Salomon, Nathan Fishkin, Luke Harris, Erin K Maloney, Yelena Kovtun, Karen Veale, Sharon D. Wilhelm, Charlene A. Audette, Juliet A Costoplus, and Ravi V.J. Chari

Bioconjugate Chem., **Just Accepted Manuscript** • DOI: 10.1021/acs.bioconjchem.5b00430 • Publication Date (Web): 10 Sep 2015

Downloaded from <http://pubs.acs.org> on September 11, 2015

Just Accepted

“Just Accepted” manuscripts have been peer-reviewed and accepted for publication. They are posted online prior to technical editing, formatting for publication and author proofing. The American Chemical Society provides “Just Accepted” as a free service to the research community to expedite the dissemination of scientific material as soon as possible after acceptance. “Just Accepted” manuscripts appear in full in PDF format accompanied by an HTML abstract. “Just Accepted” manuscripts have been fully peer reviewed, but should not be considered the official version of record. They are accessible to all readers and citable by the Digital Object Identifier (DOI®). “Just Accepted” is an optional service offered to authors. Therefore, the “Just Accepted” Web site may not include all articles that will be published in the journal. After a manuscript is technically edited and formatted, it will be removed from the “Just Accepted” Web site and published as an ASAP article. Note that technical editing may introduce minor changes to the manuscript text and/or graphics which could affect content, and all legal disclaimers and ethical guidelines that apply to the journal pertain. ACS cannot be held responsible for errors or consequences arising from the use of information contained in these “Just Accepted” manuscripts.

1
2
3
4
5
6
7
8
9
10
11
12
13
14
15
16
17
18
19
20
21
22
23
24
25
26
27
28
29
30
31
32
33
34
35
36
37
38
39
40
41
42
43
44
45
46
47
48
49
50
51
52
53
54
55
56
57
58
59
60

Title: Development of anilino-maytansinoid ADCs that efficiently release cytotoxic metabolites in cancer cells and induce high levels of bystander killing

Authors: Wayne C. Widdison*, Jose F. Ponte, Jennifer A. Coccia, Leanne Lanieri, Yulius Setiady, Ling Dong, Anna Skaletskaya, E. Erica Hong, Rui Wu, Qifeng Qiu, Rajeeva Singh, Paulin Salomon, Nathan Fishkin, Luke Harris, Erin K. Maloney, Yelena Kovtun, Karen Veale, Sharon D. Wilhelm, Charlene A. Audette, Juliet A. Costoplus, Ravi V. J. Chari

26
27
28
29
30
31
32
33
34
35
36
37
38
39
40
41
42
43
44
45
46
47
48
49
50
51
52
53
54
55
56
57
58
59
60

ABSTRACT

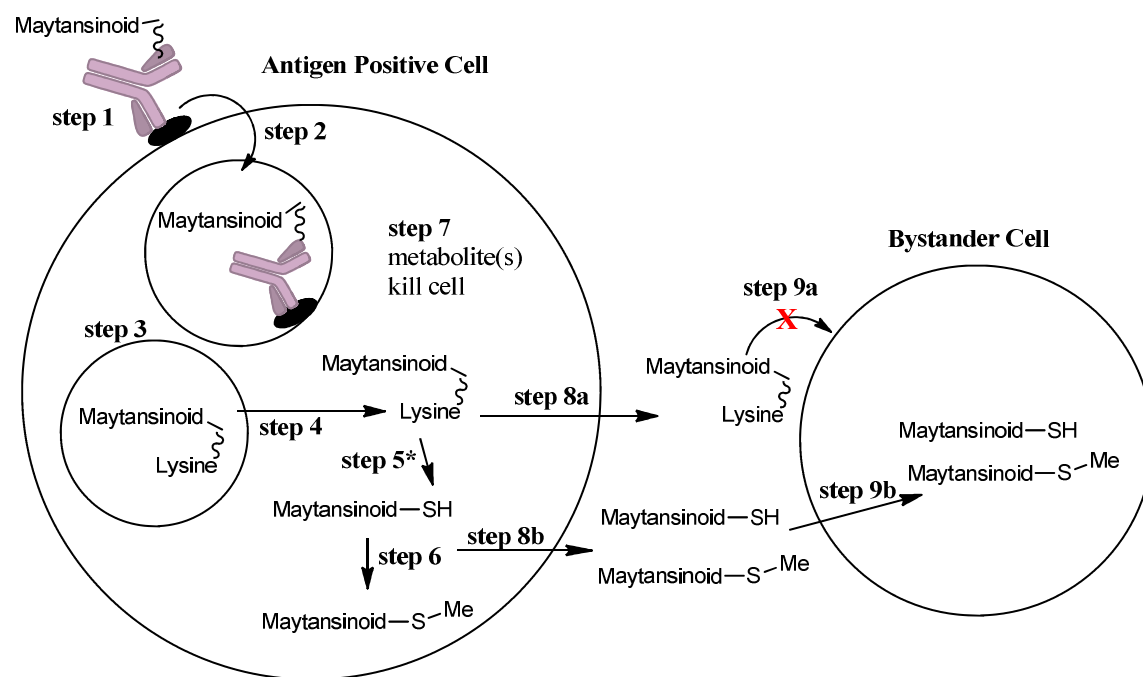
Antibody anilino maytansinoid conjugates (AaMCs) have been prepared in which a maytansinoid bearing an aniline group was linked through the aniline amine to a dipeptide which in turn was covalently attached to a desired monoclonal antibody. Several such conjugates were prepared utilizing different dipeptides in the linkage including Gly-Gly, *L*-Val-*L*-Cit and all four stereoisomers of the Ala-Ala dipeptide. The properties of AaMCs could be altered by the choice of dipeptide in the linker. Each of the AaMCs, except the AaMC bearing a *D*-Ala-*D*-Ala peptide linker, displayed more bystander killing *in vitro* than maytansinoid ADCs that utilize disulfide linkers. In mouse models, the anti-CanAg AaMC bearing a *D*-Ala-*L*-Ala dipeptide in the linker was shown to be more efficacious against heterogeneous HT-29 xenografts than maytansinoid ADCs that utilize disulfide linkers, while both types of the conjugates displayed similar tolerabilities.

INTRODUCTION

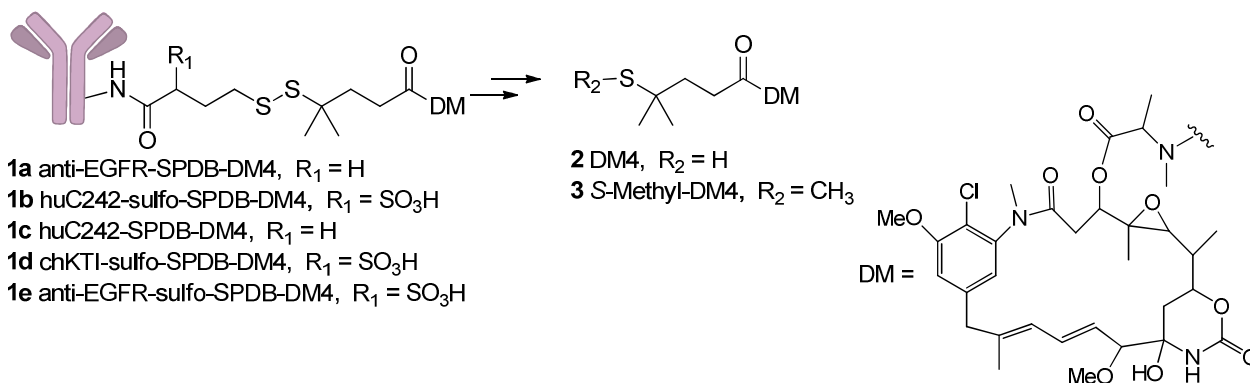
Antibody-drug conjugates (ADCs) are prepared by conjugating a cytotoxic payload to a monoclonal antibody (mAb) via a linker. All ADCs in the clinic bearing maytansinoid payloads, antibody-maytansinoid conjugates (AMCs), utilize linkers that are attached to lysine residues of the targeting antibody. The linker itself is either non-cleavable or contains a cleavable disulfide moiety. Mechanisms of how ADCs kill targeted cancer cells have been studied, and the modes by which AMCs release metabolites to kill targeted cells are depicted in Scheme 1.^{1,2} The antibody component of the AMC binds to a cancer cell in step 1. The antibody-antigen complex is internalized in step 2, traveling through one or more pre-lysosomal vesicles. In step 3, the complex is degraded in a lysosome or a pre-lysosomal vesicle until only a lysine residue of the antibody remains, attached to the unaltered maytansinoid via the linker. The initially formed metabolite is transported to the cytoplasm in step 4 and if the linker is non-cleavable, then no further degradation occurs. However, if the linker contains a disulfide bond a portion of the metabolite is cleaved in step 5 to release a thiol-bearing maytansinoid. A portion of the thiol-bearing maytansinoid can also be *S*-methylated in step 6, but with different efficiencies depending on the structure of the maytansinoid's side chain. All of the metabolites are believed to bind to microtubules and cause cells to arrest in G2/M phase before ultimately killing the cells (step 7). The lysine-bearing metabolites are charged and it is known that a significant portion can escape the cell (step 8a), however the lysine adduct cannot easily diffuse into and kill neighboring bystander cells (step 9a). The thiol-bearing and *S*-methylated maytansinoid metabolites on the other hand are not charged, and although they bind non-covalently to microtubules, they can diffuse out (step 8b) of the targeted cells and into nearby bystander cells, potentially killing them (step 9b). Thiol-bearing metabolites also have the potential to react with proteins or disulfide-containing compounds, such as cystine, in the non-reducing extracellular environment to become less membrane-permeable. Indeed the thio-maytansinoid DM4 (**2**) is several fold less potent than *S*-methylated DM4 (**3**) when tested *in vitro*.³ Also, when a thiol-bearing maytansinoid is added to buffered plasma, levels of the free thiol-bearing maytansinoid decline presumably due to formation of mixed disulfides with proteins such as albumin, or with disulfide-containing peptides. It is therefore expected that a released thio-maytansinoid would induce less bystander killing *in vivo* than a non-thiol-bearing maytansinoid such as *S*-methyl-DM4 (**3**).

Scheme 1 a) Illustration of the mechanisms by which AMC's kill cells b) Control maytansinoid conjugates used in these studies that utilize disulfide linkers and the metabolites formed from disulfide cleavage and S-methylation.

a)



b)



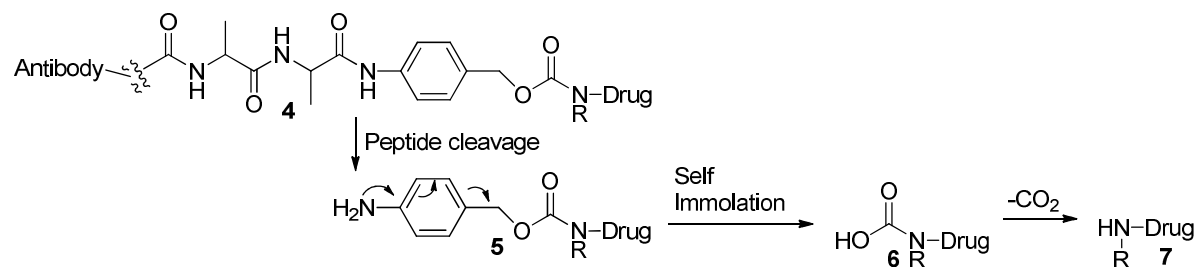
Experiments with radiolabeled antibodies indicate that a very low proportion of an injected tumor-selective antibody actually accumulates in a tumor in humans.⁴ Monoclonal antibodies to tumor-associated antigens have been reported to bind *in vivo* to cancer cells that are proximal to blood vessels but not to penetrate far from blood vessels into the tumor mass.⁵ Lower molecular weight chemotherapeutics however can penetrate more deeply into a tumor. Due to their low molecular weight, metabolites released from a cancer cell after ADC catabolism would also be

1
2
3 expected to penetrate more deeply into a tumor mass. However, only the membrane permeable
4 metabolites that can induce bystander killing can desirably diffuse into and kill these neighboring
5 cancer cells. Also ADCs with higher affinity toward an antigen are believed to have a higher
6 binding site barrier than ADCs with lower affinity.⁶⁻⁸ More of the high affinity ADCs bind to
7 cancer cells that are nearest to blood vessels so that even less ADC penetrates deeper into the
8 tumor. The cancer cells nearest to blood vessels would likely catabolize more ADC than would
9 be needed to kill them. If the released metabolites cannot induce bystander killing than much of
10 this excess killing power would not be utilized against the tumor. If the excess of released ADC
11 metabolites however can induce bystander killing than some of the neighboring cancer cells or
12 tumor stromal cells could be killed.
13
14
15
16

17
18 In many cases, tumor stromal cells have been shown to greatly aid in tumor cell growth and
19 metastasis but these cells usually do not express the antigen to which an ADC is targeted.^{9, 10}
20 Tumors often also contain cancer cells that do not express target antigen.¹¹ Thus, one would
21 expect that ADCs with bystander killing activity would be able to kill tumor stromal cells,
22 antigen-negative cancer cells, and even cells of the tumor neovasculature resulting in improved
23 anti-tumor activity. Indeed, tumor xenograft studies in mice have shown that AMCs that induce
24 bystander killing are typically several fold more efficacious than those that do not.¹¹⁻¹³
25 Conjugates utilizing the auristatin MMAE payload also display bystander killing,¹⁴ which has
26 been cited as being important for their efficacy.
27
28
29
30

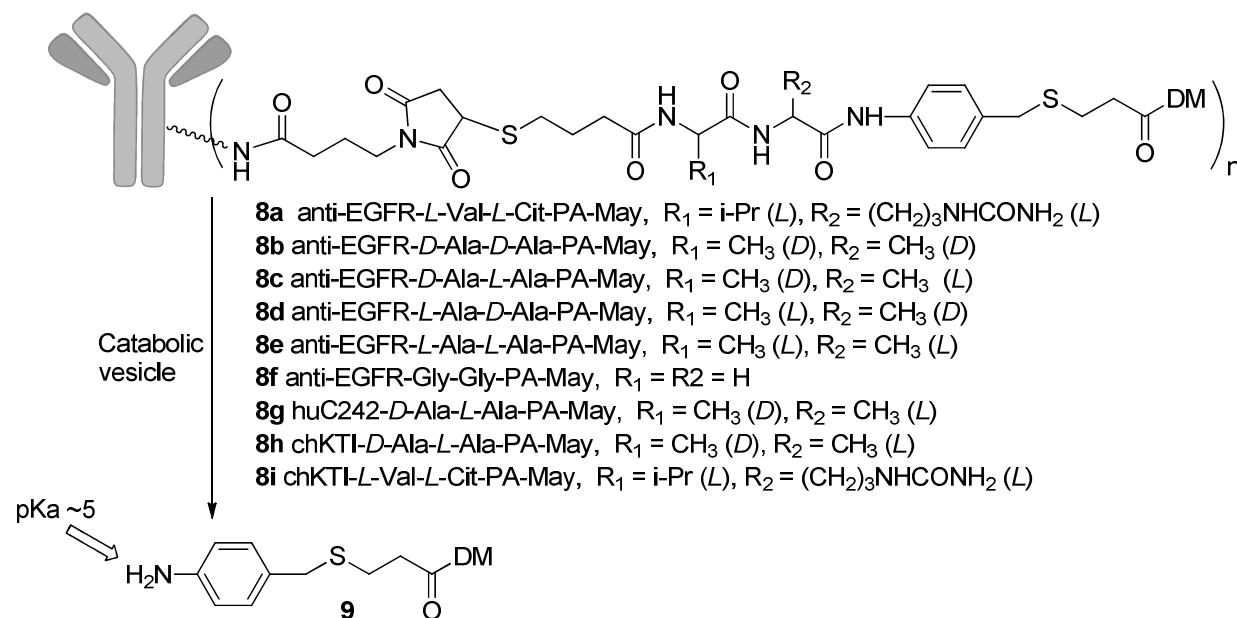
31 It may seem counter intuitive but maytansinoid ADCs that induce bystander killing are not
32 necessarily less well tolerated in humans than similar ADCs that do not induce bystander killing.
33 For example, the AMC mirvetuximab soravtansine (IMGN853), which contains a disulfide
34 linker and induces bystander killing, is dosed at approximately 6 mg/kg every three weeks in
35 current clinical testing.¹⁵ In contrast, the AMC ado-trastuzumab emtansine (Kadcyla®),
36 containing a non-cleavable linker and does not induce bystander killing, is dosed at 3.6 mg/kg
37 every three weeks in humans.^{16, 17} AMCs with disulfide linkers are catabolized to release S-
38 methylated maytansinoid, that can induce bystander killing, but reactive thio-maytansinoids, and
39 charged lysine adducts are also released, both of which may limit bystander activity. We
40 therefore wished to prepare a new type of AMC that could be efficiently degraded in endocytic
41 compartments of cells to release only non-charged, non-reactive metabolites so that even greater
42 bystander killing could be induced than is seen with AMCs that utilize disulfide linkers.
43
44
45
46
47
48
49
50
51
52
53
54
55
56
57
58
59
60

Scheme 2 Depiction of the metabolism of ADCs utilizing self immolating peptide-anilino linkages



ADCs with self-immolative linkers typically incorporate an aniline-peptide construct covalently attached through a carbamate moiety on the benzylic position of the aniline so that the released anilino compound can immolate to produce carbon dioxide and an amine-bearing cytotoxic payload.¹⁸ The amine-bearing cytotoxic payload released by this design would be mostly in a charged state below pH 9, Scheme 2. ADCs using pyrrolobenzodiazepine (PBD) dimer payloads that release a highly cytotoxic aniline-bearing PBD dimer upon cleavage of a peptide linker have been described.¹⁹ Anilines are atypical amines most often having pKa values of 5 or less, so the molecules are predominantly in a non-charged state at pH values above 5.²⁰ ADC metabolites bearing non-charged amines, such as anilines, should be more membrane permeable and thus induce a greater degree of bystander killing than metabolites bearing amines that are charged at physiological pH values. Here we describe the preparation of antibody anilino-maytansinoid conjugates (AaMCs, **8a** – **8i**) that can release an aniline-bearing maytansinoid (PA-May, **9**) upon cleavage of a peptide linker (Scheme 3). We also show results on how altering the peptide linkage affects an AaMC's metabolism, activity, and tolerability.

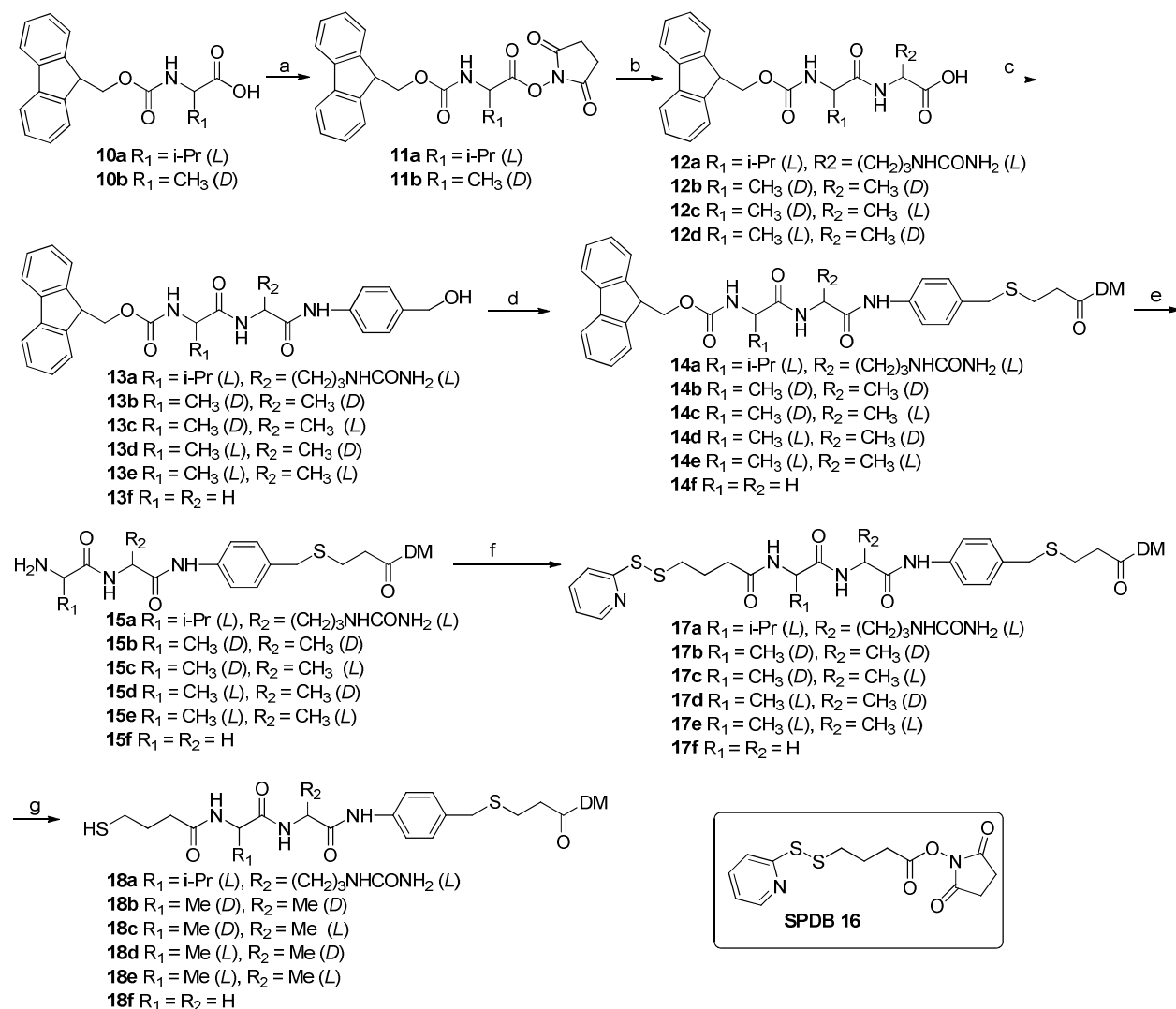
Scheme 3 Depiction of the cellular metabolism of AaMCs in a catabolic vesicle (The stereochemistry of amino acid side chains is shown in brackets)



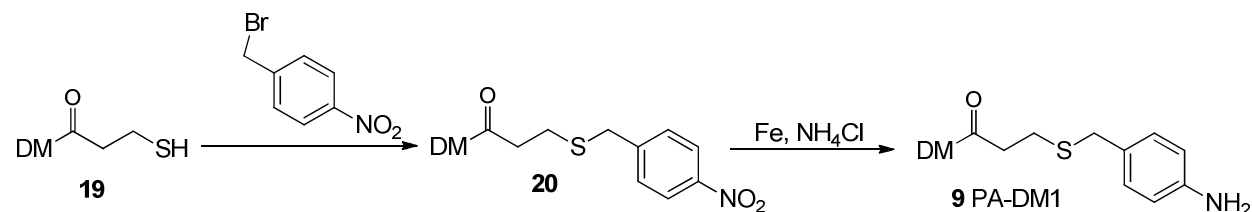
RESULTS

Synthesis of antibody maytansinoid conjugates and metabolites. AaMC precursors were prepared by the method depicted in Scheme 4. The *N*-hydroxysuccinimide (NHS) ester of the 9-fluorenylmethoxycarbonyl (Fmoc) protected amino acids (**11a-11b**) were prepared by reacting the corresponding Fmoc-protected amino acids **10a-10b** with *N*-hydroxysuccinimide (NHS) in the presence of 1-ethyl-3-(3-dimethylaminopropyl)carbodiimide HCl salt (EDC-HCl). Fmoc-protected dipeptides **12a-12d** were prepared by reacting the corresponding amino acid with the respective NHS-activated Fmoc protected amino acid **11a – 11b**. The Fmoc protected dipeptides were then reacted with 4-amino benzyl alcohol and 2-ethoxy-1-ethoxycarbonyl-1, 2-dihydroquinoline (EEDQ), as described by Dubowchik et. al., to give the compounds **13a – 13f**.¹⁸ Reaction of the individual peptides **13a – 13f** with 1 eq. of methane sulfonyl chloride in DMF followed by treatment with sodium bromide in the same pot gave the corresponding crude brominated compounds which were reacted, without isolation, with DM1 to give **14a – 14f**. The Fmoc protecting groups were removed using morpholine in DMF to give **15a – 15f**, which were each then reacted with SPDB (**16**) to give **17a-17f**. The disulfide bonds of **17a – 17f** were cleaved with 1,4-dithio-DL-threitol (DTT) to give the corresponding thio-maytansinoid **18a – 18f**. Para-anilino-maytansinoid (PA-May, **9**), the expected metabolite from cellular processing of an AaMC, was prepared in two steps by reacting DM1 (**18**) with 4-nitro-benzyl bromide in DMF to give (**19**) followed by iron catalyzed reduction of the nitro group (Scheme 5).

Scheme 4 Syntheses of AaMC maytansinoids a) NHS, EDC, b) respective amino acid, c) EEDQ, para-amino benzyl alcohol, d) Methane sulfonyl chloride, NaBr, DM1, e) morpholine, f) SPDB (16), g) DTT; The stereochemistry of amino acid side chains is shown in brackets



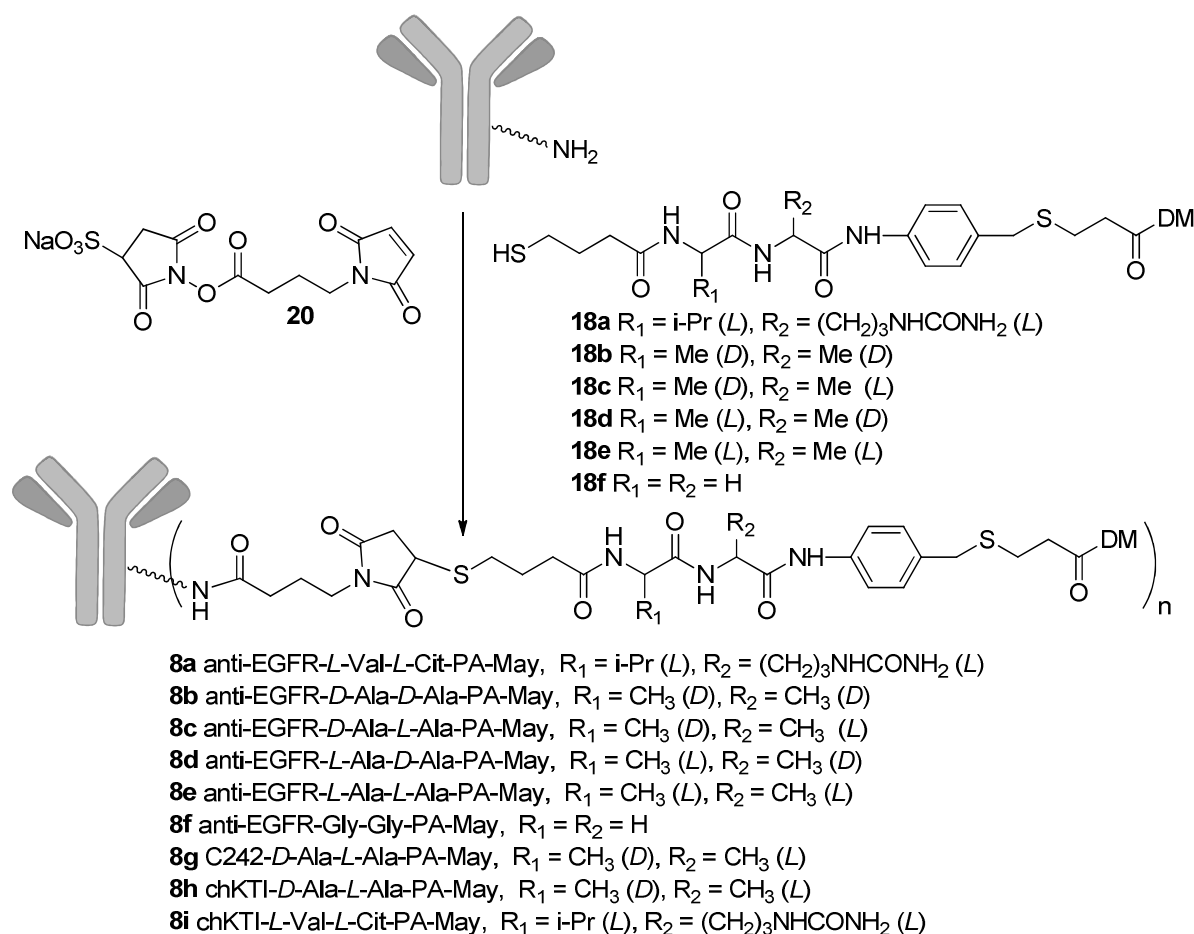
Scheme 5 Synthesis of PA-May (9)



Anti-EGFR conjugates **8a** – **8f** were prepared by conjugating a humanized anti-EGFR IgG1 antibody with the corresponding cytotoxic payloads (**17a** – **17f**) using the *N*- γ -maleimidobutyryloxysulfosuccinimide ester (sulfo-GMBS) linker (**20**) as shown in Scheme 6. The AaMC

huC242-*D*-Ala-*L*-Ala-PA-May (**8g**) was prepared in the same way but by conjugating **18c** to the humanized anti-CanAg IgG1 antibody huC242. Non-binding conjugates chKTI-*D*-Ala-*L*-Ala-PA-May (**8h**) and chKTI-*L*-Val-*L*-Cit-PA-May (**8i**), respectively, were prepared by conjugating **18c** or **18a** to a chimeric IgG1 antibody that binds to the Kunitz soybean trypsin inhibitor (chKTI). AMCs containing DM4 (**2**) conjugated to antibodies utilizing disulfide linkers: anti-EGFR-SPDB-DM4 (**1a**), huC242-sulfo-SPDB-DM4 (**1b**), huC242-SPDB-DM4 (**1c**), chKTI-sulfo-SPDB-DM4 (**1d**) and anti-EGFR-sulfo-SPDB-DM4 (**1e**) were prepared by previously described procedures; structural representations are shown in Scheme 1.²¹

Scheme 6 Conjugation of **18a** – **18f** to an antibody (anti-EGFR, COLO 205 or chKTI), with the stereochemistry of amino acid side chains shown in brackets.



In vitro cytotoxicity and bystander killing. Each of the anti-EGFR AaMCs as well as AMCs **1a** and **1e**, that utilize disulfide linkers, were assayed for their *in vitro* cytotoxicities against several EGFR+ cell lines; IC₅₀ values are recorded in Table 1. The AaMCs were more potent than conjugates **1a** and **1e** except for anti-EGFR-*D*-Ala-*D*-Ala-PA-May (**8b**). Anti-EGFR-*L*-Ala-*D*-Ala-PA-May (**8d**) was less potent than anti-EGFR-*D*-Ala-*L*-Ala-PA-May (**8c**) or anti-

EGFR AaMCs that incorporated only natural amino acids in the linker (**8a**, **8e**, **8f**). Conjugate **8c** had similar potency to anti-EGFR-*L-Ala-L-Ala-PA-May* (**8e**) and anti-EGFR-*L-Val-L-Cit-PA-May* (**8a**), against HSC2, PC9, H1975 and Ca9-22 cells, but **8a** and **8e** were more potent against SAS and OSC19 cells. A graph of the cytotoxicities of conjugates **8a**, **8c**, **8e**, and **1a** against H1975 cells is shown in Supplemental Figure S1a. The AaMCs were not always more potent than AMC that utilize disulfide linkers. For example huC242-*D-Ala-L-Ala-PA-May* (**8g**), had a similar cytotoxicity profile to huC242-SPDB-DM4 (**1c**) against CanAg-positive COLO 205 cells, while both conjugates were 100 fold less potent against CanAg-negative Namalwa cells, Supplemental Figure S1b.

Table 1 *In vitro* cytotoxicities of ADCs toward EGFR⁺ cell lines

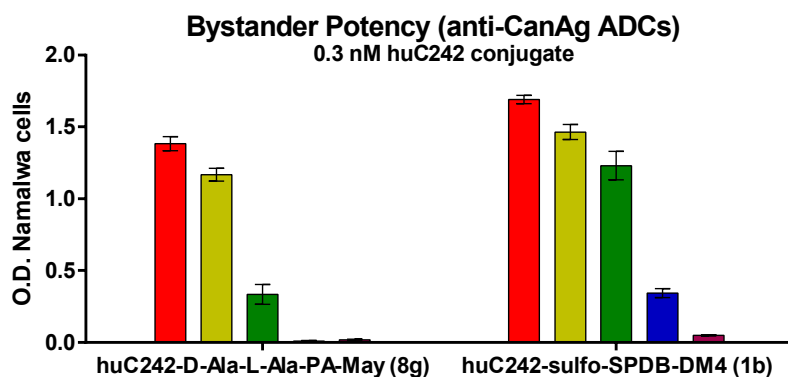
ADC	<i>In vitro</i> IC ₅₀ (nM)					
	HSC2	SAS	OSC19	PC9	H1975	Ca9-22
1a Anti-EGFR-SPDB-DM4	0.18	0.87	1.39	0.18	3.36	0.089
1e Anti-EGFR-sulfo-SPDB-DM4	0.17	3.17	3.85	4.09	4.70	0.40
8a Anti-EGFR- <i>L-Val-L-Cit-PA-May</i>	0.031	0.10	0.10	0.046	0.18	0.026
8b Anti-EGFR- <i>D-Ala-D-Ala-PA-May</i>	2.52	6.67	30.00	10.67	30.00	0.55
8c Anti-EGFR- <i>D-Ala-L-Ala-PA-May</i>	0.028	0.080	0.19	0.057	0.18	0.021
8d Anti-EGFR- <i>L-Ala-D-Ala-PA-May</i>	0.12	0.16	1.89	0.17	0.82	0.051
8e Anti-EGFR- <i>L-Ala-L-Ala-PA-May</i>	0.030	0.033	0.055	0.043	0.11	0.017
8f Anti-EGFR-Gly-Gly-PA-May	0.034	0.083	0.14	0.035	0.063	0.017

In vitro cytotoxicities were measured by WST-8 assay after a 5 day continuous exposure to the respective conjugate.

AaMCs were also tested for their capacity to induce bystander killing via an *in vitro* assay as previously described.¹¹ The assay involves incubating an ADC with a co-culture of antigen-negative and antigen-positive cells in various ratios, at a conjugate concentration that can selectively kill all antigen-positive cells, but is known not to kill any antigen-negative cells unless antigen-positive cells are present. The ADC is internalized and processed by the antigen-positive cells releasing metabolites that can kill the antigen-positive cells and any metabolites that are membrane permeable may also diffuse into and kill neighboring antigen-negative cells. ADCs that induce the most bystander killing are those that kill antigen-negative cells (bystander cells) with the lowest amount of added antigen-positive cells while keeping the ADC concentration constant (bystander killing method 1). Bystander killing of anti-CanAg conjugates was evaluated by method 1 using 5000 antigen-negative Namalwa cells in the presence of different numbers of antigen-positive COLO 205 cells and 0.3 nM of either huC242-*D-Ala-L-Ala-PA-May* (**8g**), or huC242-sulfo-SPDB-DM4 (**1b**), Figure 1a. AMC **1b** required the addition of 625 COLO 205 cells to induce over 50% bystander killing and **8g** was approximately twice as efficient as **1b**, requiring only 250 COLO 205 cells to induce over 50% bystander killing. In a

1
2
3 separate experiment huC242- SPDB-DM4 (**1c**) was found to have the same degree of bystander
4 killing as conjugate **1b** while a conjugate utilizing a non-cleavable linker displayed no bystander
5 killing (data not shown). In a similar bystander killing assay (method 2) a fixed number of
6 antigen-negative cells were incubated with a fixed amount of antigen-positive cells in the
7 presence of an ADC at a single concentration. Anti-EGFR AaMCs were assayed for bystander
8 killing via method 2 using 2000 antigen-negative cells (MCF7) and 3000 antigen-positive cells
9 (Ca9-22) in the presence of either anti-EGFR-*L*-Val-*L*-Cit-PA-May (**8a**), anti-EGFR-*D*-Ala-*L*-
10 Ala-PA-May (**8c**), anti-EGFR-*L*-Ala-*D*-Ala-PA-May (**8d**), anti-EGFR-*L*-Ala-*L*-Ala-PA-May
11 (**8e**) at a concentration of 0.66 nM or with no added conjugate, Figure 1b. AaMCs **8a**, **8c** and **8e**
12 displayed similar levels of bystander killing while **8d** had slightly lower bystander killing. In a
13 separate experiment anti-EGFR-*D*-Ala-*D*-Ala-PA-May (**8b**) was shown to have essentially no
14 bystander killing (data not shown). For either bystander killing method, the number of antigen
15 positive cells required depends on their output of metabolite, which in turn depends on their
16 target antigen density and ADC processing efficiency.
17
18
19
20
21
22
23
24
25
26
27
28
29
30
31
32
33
34
35
36
37
38
39
40
41
42
43
44
45
46
47
48
49
50
51
52
53
54
55
56
57
58
59
60

a)



Number of antigen-positive COLO 205 cells ■ None, ■ 125, ■ 250, ■ 625, ■ 1250

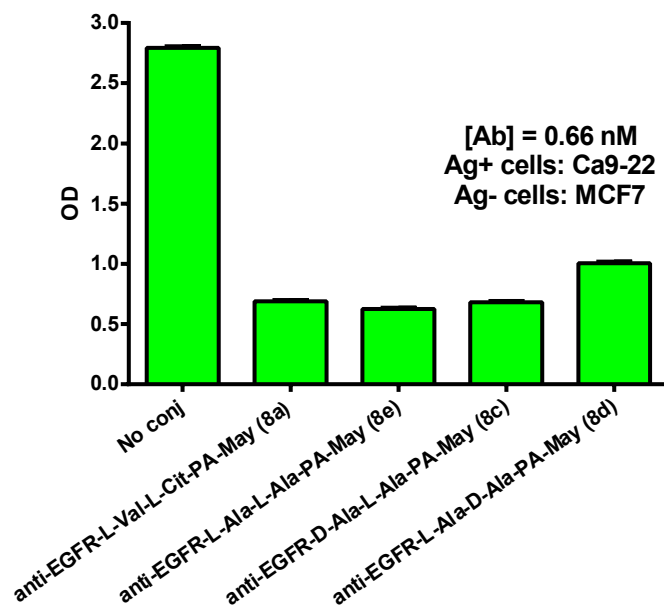
b) **Bystander Potency (anti-EGFR AaMCs)**

Figure 1 Bystander killing assay in which 5000 antigen-negative cells (Namalwa) were mixed with the following number of COLO 205 cells: none ■, 125 ■, 250 ■, 625 ■, or 1250 ■ and the mixtures were treated with anti-CanAg conjugates (**1b**, or **8g**) at a concentration of 0.3 nM. b) Bystander killing assay in which 2000 antigen-negative cells (MCF7) were mixed with 3000 antigen-positive cells (Ca9-22) and the mixtures were either treated with the indicated conjugate at a concentration of 0.66 nM, or not treated (control). Relative cell numbers were determined by the WST-8 assay.

1
2
3
4
5
6
7
8
9
10
11
12
13
14
15
16
17
18
19
20
21
22
23
24
25
26
27
28
29
30
31
32
33
34
35
36
37
38
39
40
41
42
43
44
45
46
47
48
49
50
51
52
53
54
55
56
57
58
59
60

Inhibition of AaMC induced G2/M cell cycle arrest by Bafilomycin A1. Studies were undertaken to determine if any of the AaMCs could induce cell cycle arrest in the G2/M phase if endosomal transport to lysosomal vesicles was blocked. Bafilomycin A1 (Baf A1) selectively inhibits V-ATPase, a proton pump present in endosomes and lysosomes, which leads to neutralization of the pH in these vesicles.²² The pH neutralization blocks trafficking from late endosomes to lysosomes and lysosomal processing, but only modestly affects the rate of internalization and recycling and does not inhibit trafficking between endosomes and trans-Golgi.²³ These experiments showed that G2/M phase cell arrest occurred when EGFR-positive cells were treated with cell-targeting anti-EGFR AaMCs (**8a** – **8f**) (Supplemental Figure S2). Cell arrest was blocked by Baf A1 for anti-EGFR-Gly-Gly-PA-May (**8f**) and for AaMCs **8b-8d**, which contain at least one *D*-Alanine in the linker. However the AaMCs that contained only *L*-amino acids in the linkage (**8a** and **8e**) retained between 50 - 80 % of their ability to arrest cells in the presence of Baf A1.

23
24
25
26
27
28
29
30
31
32
33
34
35
36
37
38
39
40
41
42
43
44
45
46
47
48
49
50
51
52
53
54
55
56
57
58
59
60

Identification of the major metabolite of AaMCs. Two experiments were conducted to identify which metabolite(s) could be generated by catabolism of AaMCs. First anti-EGFR-*L*-Val-*L*-Cit-PA-May (**8a**) was incubated with cathepsin B at 37 °C, followed by HPLC/MS analysis. One major product was formed and was shown to have the same HPLC retention time and MS profile as the synthetic standard PA-May (**9**), Figure 2a. In a second experiment huC242-*D*-Ala-*L*-Ala-PA-May (**8g**) was incubated with COLO 205 cells *in vitro* for 24 h after which the cells were pelleted, lysed and analyzed by HPLC/MS, Figure 2b. A control of untreated COLO 205 cells was also analyzed by HPLC/MS, Figure 2c. A major HPLC peak (retention time 26.6 – 27 min) was seen in the test sample but not in the control sample. This new peak had the same retention time and mass spectrum as PA-May **9**, indicating that **9** is a major metabolite of **8g** in COLO 205 cells. The mass spectrum for **9** is shown in Supplemental Figure S3.

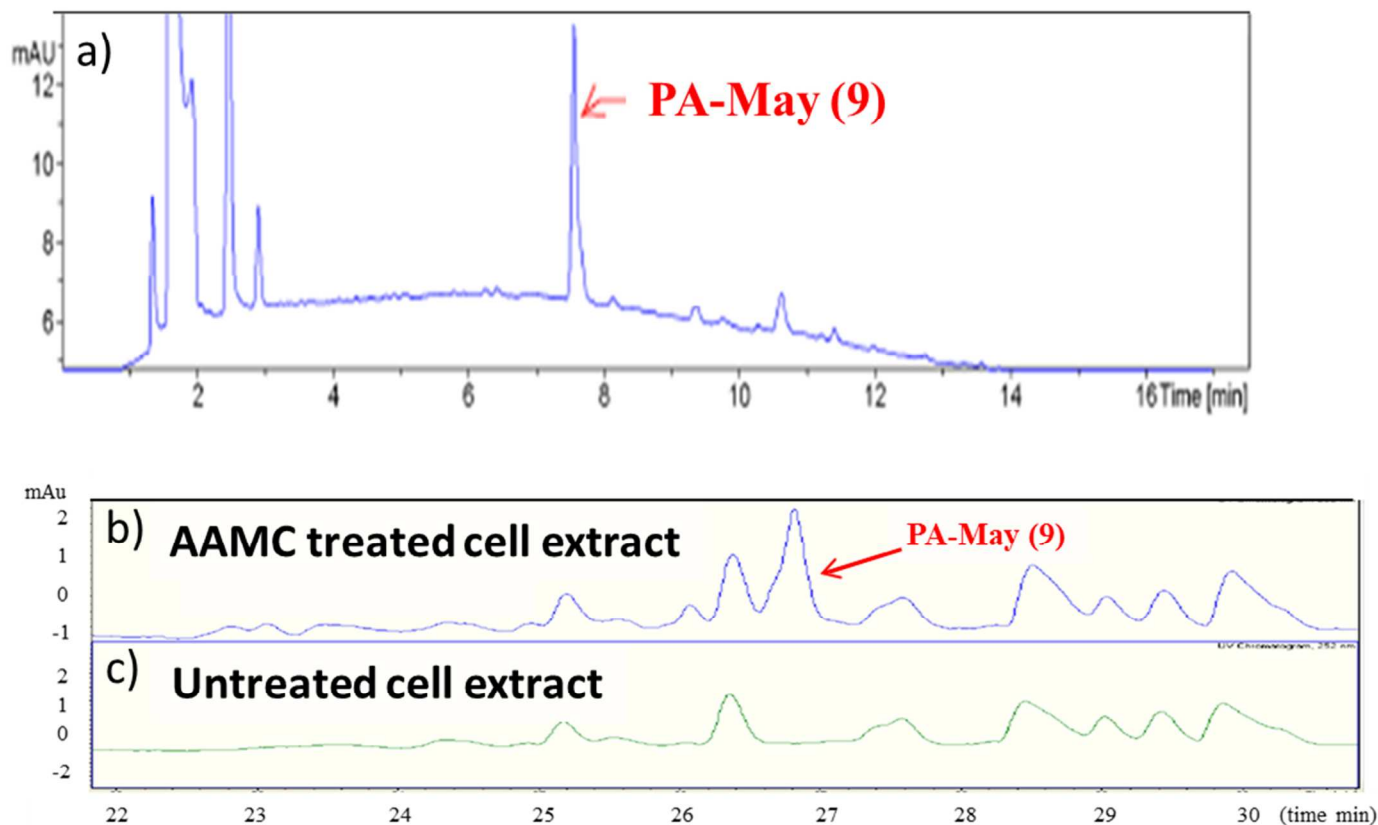


Figure 2 HPLC traces of a) Cathepsin B treated anti-EGFR AaMC 8a analyzed using analytical HPLC method 1 and b) Lysate from anti-CanAg AaMC 8g treated COLO 205 cells (AaMC cell extract), analyzed by analytical HPLC method 2 c) lysed COLO 205 cells that were not exposed to any conjugate (untreated cell extract), analyzed by analytical HPLC method 2.

Quantitation of metabolite produced by anti-EGFR AaMC 8c and anti-EGFR AMC 1a.

EGFR-expressing HSC2 cells were incubated with anti-EGFR-SPDB-DM4 (**1a**) or anti-EGFR-*D*-Ala-*L*-Ala-PA-May (**8c**) for 2 h after which cells were washed then allowed to process internalized ADC for 24 h. Over this time frame it is known that cells remain alive and membranes are not ruptured to release cellular contents into the cell media. The amount of metabolite in organic extracts of cells and in unextracted media were determined using an anti-maytansinoid binding competition ELISA, Supplemental Figure S4.²⁴ Incubations with conjugate **8c** produced approximately 25% more total metabolite than conjugate **1a**. Incubations with **8c** also released approximately twice as much metabolite into the cell media as that with **1a**. HSC2 cells however retained similar amounts of metabolite from the **8c** and **1a** incubations.

1
2
3 ***In vitro* cytotoxicity of the anilino-maytansinoid AaMC metabolite 9.** The cytotoxicity of
4 synthesized PA-May (**9**) was determined on KB cells and found to be similar to *S*-methyl-DM4
5 (**3**), the most cytotoxic metabolite of DM4 bearing AMCs; $IC_{50} = 7.0 \times 10^{-11}$ and 6.0×10^{-11} for **9**
6 and **3** respectively.
7
8

9
10 **Determination of the MTD of AaMCs in mice.** Pilot studies were conducted with 3 mice per
11 group to determine the approximate maximum tolerated dose (MTD) of selected conjugates, with
12 dosing based on linked maytansinoid. The MTD was considered reached for a given group when
13 at least one mouse of that group lost 20% or more of its pre-treatment weight or upon
14 observations of any clinical signs of distress. Each of the conjugates utilized an anti-EGFR
15 antibody that does not cross react with murine EGFR. AaMCs anti-EGFR-*L*-Val-*L*-Cit-PA-May
16 (**8a**) and anti-EGFR-Gly-Gly-PA-May (**8f**) had the lowest MTDs, both approximately 900 $\mu\text{g}/\text{kg}$
17 based on maytansinoid dose. AaMC anti-EGFR-*L*-Ala-*L*-Ala-PA-May (**8e**) was not tolerated at
18 1,400 $\mu\text{g}/\text{kg}$ but the other AaMC containing alanine residues in the linkage (**8b**, **8c** and **8d**) were
19 tolerated at this dose (see Supplemental Figure S5). This preliminary MTD was in line with
20 MTDs previously determined for AMCs that utilize disulfide linkers.¹² Since anti-EGFR-*D*-Ala-
21 *L*-Ala-PA-May (**8c**) was the most potent of the well tolerated AaMCs, *D*-Ala-*L*-Ala was selected
22 as the lead dipeptide moiety for AaMCs. A second MTD study was conducted with chKTI-*D*-
23 Ala-*L*-Ala-PA-May (**8h**) and chKTI-sulfo-SPDB-DM4 (**1d**) using a larger number of animals (9
24 mice per group) for comparison, Figure 3. Mice were dosed with **8h** at 1000, 1250 and 1500
25 $\mu\text{g}/\text{kg}$ and **1d** was dosed at 1500 $\mu\text{g}/\text{kg}$. Neither conjugate was tolerated at 1500 $\mu\text{g}/\text{kg}$, however
26 the averaged weight loss was similar for the two conjugates at this dose. The MTD of **8h** was
27 found to be between 1000 – 1250 $\mu\text{g}/\text{kg}$.
28
29
30
31
32
33
34
35
36
37
38
39
40
41
42
43
44
45
46
47
48
49
50
51
52
53
54
55
56
57
58
59
60

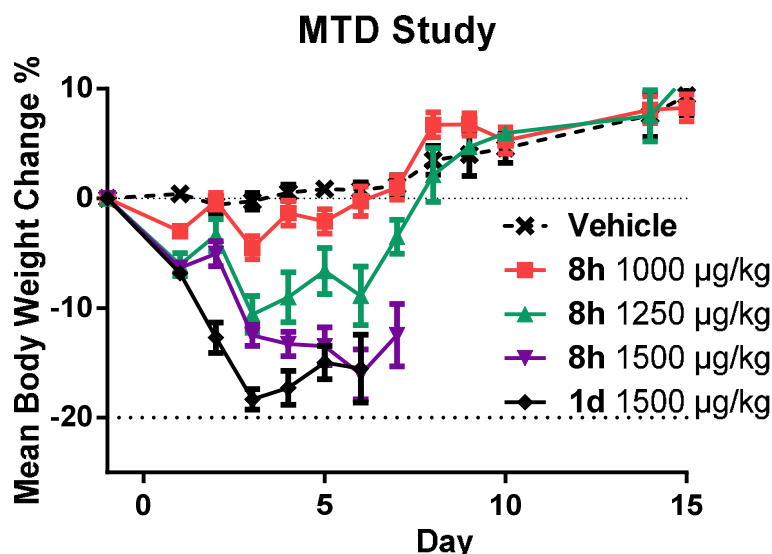
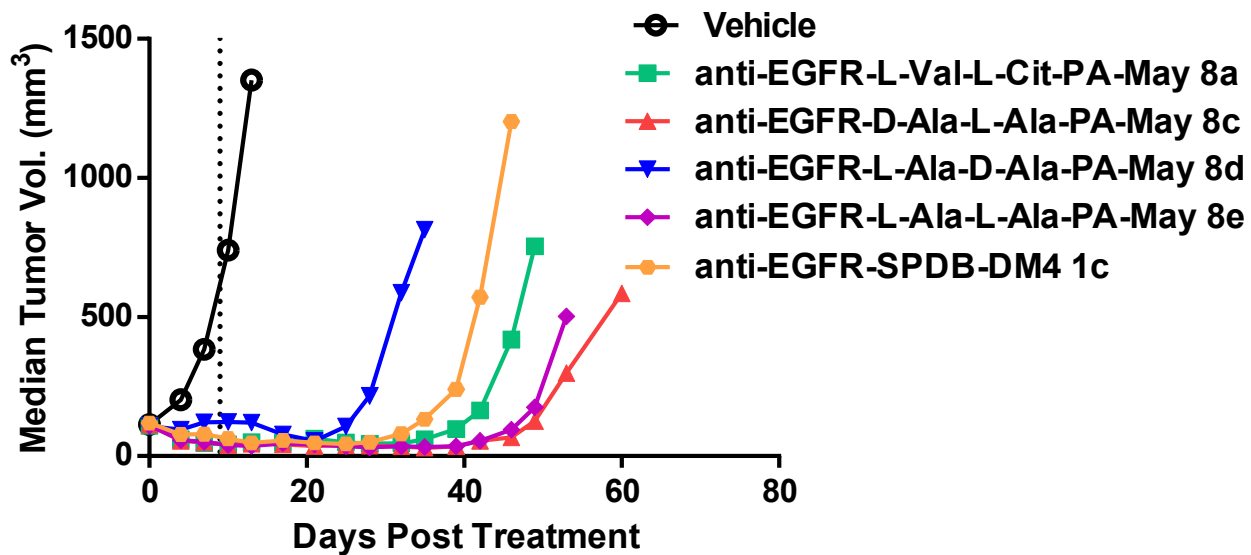


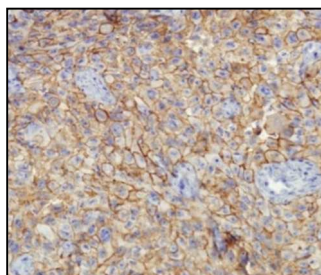
Figure 3 Maximum tolerated dose (MTD) study of chKTI-*D*-Ala-*L*-Ala-PA-May **8h** compared to chKTI-sulfo-SPDB-DM4 **1d**.

In vivo efficacy of AaMCs. The AaMCs anti-EGFR-*L*-Val-*L*-Cit-PA-May (**8a**), anti-EGFR-*D*-Ala-*L*-Ala-PA-May (**8c**), anti-EGFR-*L*-Ala-*D*-Ala-PA-May (**8d**), and anti-EGFR-*L*-Ala-*L*-Ala-PA-May (**8e**) were tested for efficacy in mice bearing H1975 xenografts, Figure 4a. H1975 xenografts displayed high homogeneous expression of EGFR, determined by immunohistochemical analysis, Figure 4b. Anti-EGFR-SPDB-DM4 (**1a**) was also evaluated in this study for comparison. The tumor size ratio (T/C) indicates the median tumor size of the test group divided by the median tumor size for the control group.²⁵ The tumor growth delay (T-C) indicates the time in days that it took for the median tumor size of a test group to reach 678 mm³ minus the time in days it took for the median tumor size of the control group to reach the same size. 678 mm³ was the maximum median tumor size achievable for all groups in this study, mice that did not regrow tumors were not included in the (T-C) calculation. Most of the conjugates were highly active at 3 mg/kg. Anti-EGFR-*L*-Ala-*D*-Ala-PA-May (**8d**) had a T/C of 12% and the shortest T-C (33 days). All other AaMCs showed similar T/C (2-4%) and T-C (~55 days) values and had longer T-C values than the anti-EGFR-SPDB-DM4 (**1a**) (42 days). In a separate study anti-EGFR-Gly-Gly-PA-May (**8f**) and anti-EGFR-*L*-Val-*L*-Cit-PA-May (**8a**) showed similar efficacy at 3 mg/kg in mice bearing H1975 xenografts (data not shown).

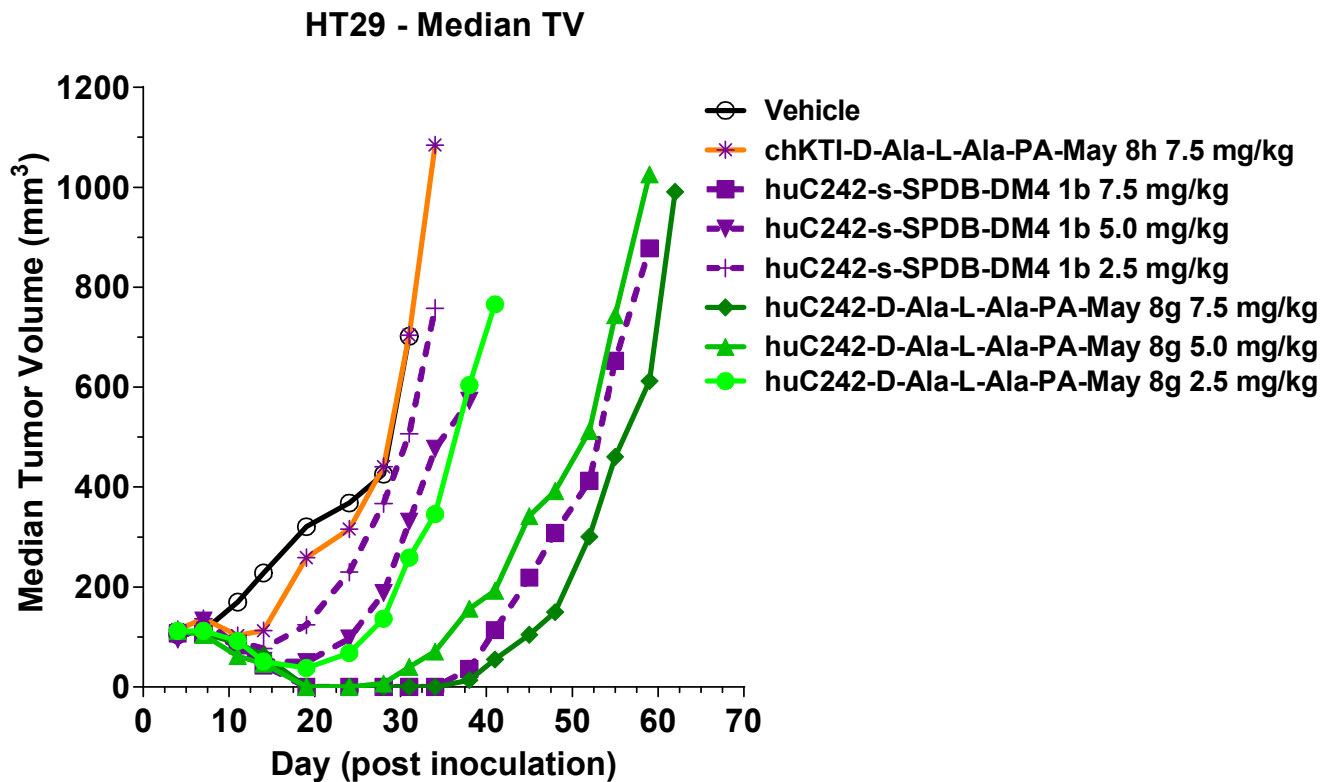
a) Homogeneous H1975 Xenograft Model



b)



c) Heterogeneous HT-29 Xenograft Model



	%T/C	ACTIVITY	Regressions	
			PR	CR
Vehicle	-	-	-	-
chKTI-D-Ala-L-Ala-PA-May 8h (7.5 mg/kg)	100%	Inactive	0/6	0/6
huC242-sulfo-SPDB-DM4 1c (7.5 mg/kg)	0%	Highly Active	6/6	6/6
huC242-sulfo-SPDB-DM4 1c (5.0 mg/kg)	47%	Inactive	4/6	2/6
huC242-sulfo-SPDB-DM4 1c (2.5 mg/kg)	72%	Inactive	1/6	0/6
huC242-D-Ala-L-Ala-PA-May 8g (7.5 mg/kg)	0%	Highly Active	6/6	6/6
huC242-D-Ala-L-Ala-PA-May 8g (5.0 mg/kg)	6%	Highly Active	6/6	4/6
huC242-D-Ala-L-Ala-PA-May 8g (2.5 mg/kg)	37%	Active	4/6	1/6

d)

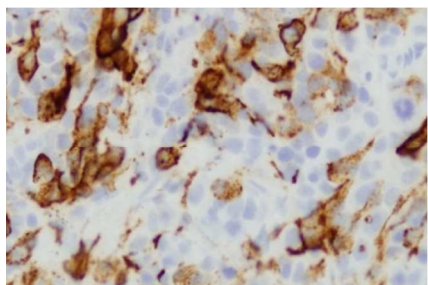


Figure 4 Efficacy of AaMCs against homogeneous and heterogeneous tumor xenografts in mice a) SCID mice (6 mice/group) bearing homogeneous H1975 NSCLC xenografts were treated with a single intravenous dose of PBS or 3 mg/kg of the following (○); anti-EGFR-*L*-Val-*L*-Cit-PA-May **8a** (■); anti-EGFR-*D*-Ala-*L*-Ala-PA-May **8c** (▲); anti-EGFR-*L*-Ala-*D*-Ala-PA-May **8d** (▼); anti-EGFR-*L*-Ala-*L*-Ala-PA-May **8e** (◆); anti-EGFR-SPDB-DM4 **1a** (●) b) Staining for EGFR on H1975 xenograft showing 2-3 Homogeneous expression c) SCID mice (6 mice/group) bearing heterogeneous HT-29 xenografts that were treated with a single intravenous dose of PBS (○); or 7.5 mg/kg mAb-*D*-Ala-*L*-Ala-PA-May **8h** (*); 7.5 mg/kg huC242-SPDB-DM4 **1c** dashed line (■); 5.0 mg/kg huC242-SPDB-DM4 **1c** dashed line (▼); 2.5 mg/kg huC242-SPDB-DM4 **1c** dashed line (+); 7.5 mg/kg huC242-*D*-Ala-*L*-Ala-PA-May **8g** (◆); 5.0 mg/kg huC242-*D*-Ala-*L*-Ala-PA-May **8g** (▲); 2.5 mg/kg huC242-*D*-Ala-*L*-Ala-PA-May **8g** (●). %T/C was calculated as the median tumor volume of treated groups (T) divided by the median tumor volume of the vehicle control group (C) and activity was assigned according to the National Cancer Institute standards (%T/C ≤ 42% = active, %T/C ≤ 1% = highly active. PR indicates partial regression (greater than 50% reduction of tumor xenograft size) CR indicates complete regression (tumor xenograft no longer detected). d) Staining of CanAg on HT-29 Xenograft showing 3 heterogeneous expression.

An efficacy study in mice bearing HT29 xenografts was done to assess the activity of a huC242-*D*-Ala-*L*-Ala-PA-May (**8g**) in comparison to huC242-sulfo-SPDB-DM4 (**1b**) (Figure 4c). Expression of CanAg antigen in HT29 xenografts is highly heterogeneous, with staining for the antigen seen on only a small subset of HT29 cells (Figure 4d), thus providing a model to assess bystander potency.¹¹ Conjugates **8g** and **1b** were administered i.v. with dosings of 2.5 mg/kg, 5.0 mg/kg or 7.5 mg/kg. The **1b** conjugate was highly active at 7.5 mg/kg with a T/C of 0% and 6/6 partial regressions (PRs) and complete regressions (CRs), but had little activity at the 2.5 mg/kg dose (T/C 72%; 0/6 CR). The **8g** conjugate was active at 2.5 mg/kg (T/C = 37% with 4/6 PR and 1/6 CR) and highly active at 5 and 7.5 mg/kg (T/C 6 and 0%, 6/6 and 6/6 PR, and 4/6 and 6/6 CR, respectively). The minimally efficacious dose of **8g** in this study was 2.5 mg/kg compared to about 5.0 mg/kg for the **1b** conjugate. The non-targeting AaMC **8h** was inactive at 7.5 mg/kg, indicating that the efficacy of **8g** was specifically targeted.

Pharmacokinetics of anti-EGFR-*D*-Ala-*L*-Ala-PA-May **8c in mice.** Six mice were administered a single 10 mg/kg i.v. dose of anti-EGFR-*D*-Ala-*L*-Ala-PA-May (**8c**). The concentration of the antibody component of the conjugate and the concentration of intact maytansinoid-bearing conjugate from mouse blood samples were determined by ELISA as previously described.²⁶ The ELISA involves the capture of conjugate bearing at least one attached maytansinoid using an anti-maytansinoid antibody then the antibody component of the conjugate is captured and detected with an enzyme labeled anti-FC antibody. In order to be detected a conjugate must contain at least one covalently linked maytansinoid. The total antibody, antibody bearing at least one maytansinoid as well as antibody with no attached maytansinoids, is determined by capturing it with an anti-human IgG antibody then quantitated

using an enzyme labeled anti-human IgG antibody. Results of the study are shown in Figure 5. The PK parameters for the antibody component of the conjugate were as follows; C_{max} of 190 $\mu\text{g/mL}$, $T_{1/2}$ of 12.3 days, $AUC_{0-\infty}$ 25,960 $\text{h}^* \mu\text{g/mL}$, Cl of 0.39 mL/h/kg and a V_{ss} of 153.9 mL/kg . These parameters are in similar to observed PK parameters for the naked antibody in mice, suggesting that conjugation had little effect on the PK parameters of the antibody component of this conjugate. The PK parameters for the intact maytansinoid-bearing conjugate were as follows; C_{max} 225 $\mu\text{g/mL}$, $T_{1/2}$ of 5 days, $AUC_{0-\infty}$ 11,969 $\text{h}^* \mu\text{g/mL}$, Cl of 0.84 mL/h/kg and a V_{ss} of 158.0 mL/kg . These parameters are in line with observed PK parameters for typical disulfide linked DM4 conjugates, where the $T_{1/2}$ for the overall clearance of the intact conjugates were also about 5 days.²⁷

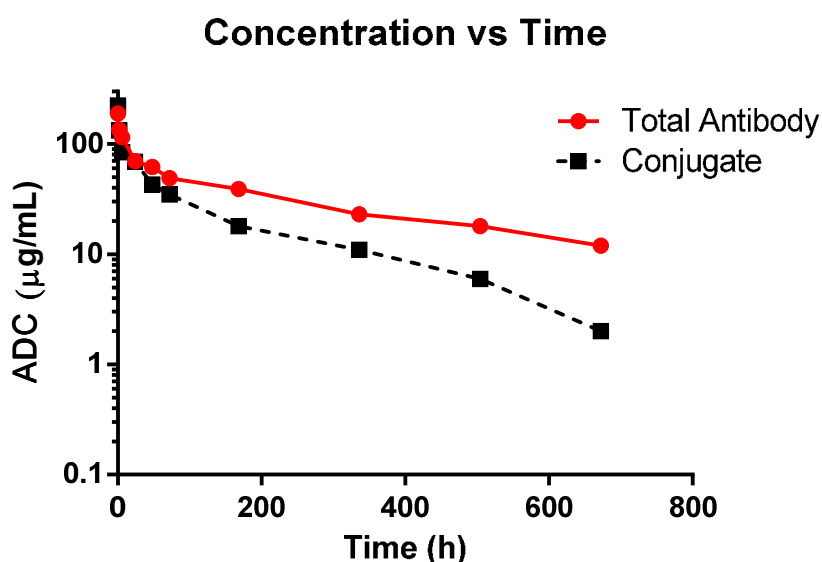


Figure 5 *In vivo* clearance rate of anti-EGFR-*D*-Ala-*L*-Ala-PA-May (**8c**) in mice. The ● graph indicates the concentration versus time plot of the antibody component of **8c**, the ■ graph indicates the concentration versus time plot of the maytansinoid component of **8c**. Concentrations were determined by two ELISA assays which separately quantitate antibody and conjugate that contains at least one maytansinoid.

DISCUSSION

A new class of maytansinoid-based ADC has been prepared that can release an aniline-bearing maytansinoid, via cleavage of a peptide linker. The metabolite PA-May **9** is highly cytotoxic to the cell in which it is formed and because it is predominantly non-charged, it can diffuse into neighboring cells to induce greater bystander killing than is achieved with AMCs that release charged or reactive metabolites such as AMCs with sulfo-SPDB linkers (Figure 1a). The type of di-peptide used in an AaMCs linker can affect the conjugates ability to induce bystander killing

1
2
3 or to be inhibited by Bafilomycin A1. For example, in cases where a *D*-Alanine residue is linked
4 directly to the aniline amine (Table 1 and Figure 1b) poorer bystander killing is noted. It is
5 likely that a portion of these AaMCs does not undergo cleavage of the dipeptide linker, in which
6 case one or more charged metabolites that do not induce bystander killing, would be released.
7 However, a *D*-alanine residue can be incorporated into the dipeptide of the linker without
8 impairing the AaMCs cytotoxicity, against most of the tested cell lines, as long as an *L*-alanine is
9 attached directly to the aniline moiety. The presence of a *D*-amino acid in either position of an
10 AaMCs linker or linkers having two glycines caused cytotoxicity to be blocked in the presence
11 of Bafilomycin A1, indicating the need for linker cleavage in lysosomes. The cytotoxicity of
12 AaMCs utilizing only *L*-amino acids in the linkage however was only partially inhibited by
13 Bafilomycin A, indicating that the peptide linkages could be cleaved with 50% or higher
14 efficiency in pre-lysosomal compartments of the tested cells. AaMCs only require the cleavage
15 of a single bond in their peptide linker to release the metabolite PA-May (**9**). In contrast, AMC
16 with disulfide linkers require multiple bonds of the antibody to be cleaved in order to release an
17 initial metabolite, which may be less efficient. Indeed we have seen that some targeted cells can
18 release more total metabolite from an optimized AaMC than from an AMC bearing a disulfide
19 linker.
20
21
22
23
24
25
26

27 Pharmacokinetic studies indicate that the AaMC bearing the *D*-Ala-*L*-Ala dipeptide linker (**8c**)
28 has a similar clearance rate in circulation in mice as that reported for disulfide-linked DM4
29 conjugates.¹² Both types of conjugate displayed loss of maytansinoid payload from the antibody
30 component, but only slowly and at approximately the same rate, for an overall conjugate T1/2 of
31 about 5 days. Conjugates containing payloads linked to a maleimide via a thio-ether are known
32 to slowly release the payload in the presence of thiols.^{28, 29} The half life of a maytansinoid
33 conjugate with a maleimide thio-ether linkage is only about 30 h longer than that of SPDB linked
34 DM4 conjugates, while AMCs that utilize highly hindered disulfide linkages that are very stable
35 have half lives of over 9 days.¹² So it is likely that a large portion of the maytansinoid released
36 from **8c** *in vivo* was due to thio-ether cleavage but some maytansinoid loss was probably also due
37 to cleavage of the peptide linker. Anti-EGFR-*D*-Ala-*L*-Ala-PA-May (**8c**) was better tolerated in
38 mice than anti-EGFR-*L*-Ala-*L*-Ala-PA-May (**8e**). This may be due to differences in the stability
39 of the dipeptide linkages of these AaMCs during circulation in mice and will require further *in*
40 *vivo* PK studies.
41
42
43
44
45
46

47 The anti-EGFR AaMCs were efficacious against homogeneously expressing H1975 xenografts
48 and most were slightly more efficacious than anti-EGFR-SPDB-DM4 (**1a**). Anti-EGFR-*L*-Ala-
49 *D*-Ala-PA-May (**8d**) was the least efficacious of the tested AaMCs, and this AaMC showed
50 lower cytotoxicity and lower bystander killing than AaMCs bearing an *L*-amino acid attached to
51 the aniline. As previously stated this could be due to less efficient cleavage of the peptide linker
52 of the conjugate resulting in the release of less total metabolite. Also partial cleavage of the
53 peptide linker of **8d** would give a positively charged metabolite that still contained the *D*-alanine
54 residue of the linker, which would presumably have poor bystander killing. If a portion of the
55
56
57
58
59
60

1
2
3 conjugate did not undergo cleavage of the peptide linker, then metabolites bearing a lysine
4 residue or a larger peptide fragment derived from the antibody would be released. These lysine
5 or peptide bearing metabolites would not be expected to induce bystander killing and their ability
6 to diffuse from the catabolic vesicle into the cytoplasm of the cell might be impaired. When the
7 antigen is expressed in a heterogeneous manner, such as in HT-29 xenografts, the AaMC,
8 huC242-*D*-Ala-*L*-Ala-PA-May (**8g**) was substantially more efficacious than the corresponding
9 AMC bearing a disulfide linker (huC242-sulfo-SPDB-DM4 **1b**). In vivo efficacy studies using
10 xenografts composed of a mixture of antigen-positive and antigen-negative cells in various ratios
11 have been reported.³⁰ Similar mixed xenograft efficacy studies would be of value in future work
12 to more exactly determine the percent of antigen positive cells required for *in vivo* efficacy
13 against heterogenous xenografts.
14
15
16
17
18

19 Efficacy studies on heterogeneous xenografts may better mimic the treatment of tumors in
20 patients for several reasons. Antigen expression in human tumors often varies and may not
21 always be as homogeneous as EGFR expression in H1975 xenografts. Reports also indicate that
22 mouse stroma secretes mouse cytokines and growth factors that in many situations do not aid the
23 survival and promotion of metastasis of human cancer cells as effectively as those secreted from
24 human stroma.³¹⁻³³ Many types of human cancer cells however secrete growth factors and
25 cytokines.^{34, 35} So non-targeted antigen-negative cancer cells in a heterogeneous xenograft might
26 take on some of the role human tumor stroma plays in aiding cancer cells to survive. AaMCs are
27 a promising new class of maytansinoid conjugate, which may be well suited for killing a
28 patient's cancerous cells as well as the tumor stromal cells that support cancer cell survival. The
29 studies described herein should also be of use in the design of ADCs that utilize peptide linkages
30 to non-maytansinoid payloads.
31
32
33
34
35
36
37
38
39
40
41
42
43
44
45
46
47
48
49
50
51
52
53
54
55
56
57
58
59
60

EXPERIMENTAL

All reagents were obtained from Chem Impex, Bachem, or Sigma-Aldrich unless otherwise stated. All synthetic reactions were conducted under an argon atmosphere with magnetic stirring unless otherwise stated. Proton magnetic resonance (^1H NMR) and carbon magnetic resonance spectra (^{13}C NMR) were obtained on a Bruker Avance 400 spectrometer operating at 400 MHz and 100 MHz respectively. In cases where ^{13}C NMRs were taken using DMSO- d_6 as the solvent, a small amount of CDCl_3 was also added. The NMR chemical shifts are reported in δ values relative to the utilized NMR solvent. Centrifugations whether under vacuum or without vacuum were performed on a Thermo electron SPD SpeedVac equipped with a UVS800DDA universal vacuum system. Lyophilizations were performed using a VerTis Benchtop K. Flash chromatography was performed on an Agilent Intelliflash system. HPLC purifications were performed using Gilson 334 pumps in series with a Gilson UV/Vis-156 dual wavelength detector and a Gilson FC204 fraction collector. High resolution mass spectra were obtained on a Thermo Fisher Q-Exactive instrument. Analytical HPLC/MS data was obtained on an Agilent 1100 HPLC in series with a Bruker esquire 3000 ion trap MS operating in alternating positive/negative ion mode or on an Agilent 1260 HPLC in tandem with an Agilent 6120 single quadrupole mass spectrometer. Fmoc-*L*-Val-*L*-Cit-OH and Fmoc-*L*-Val-*L*-Cit-PA-OH were prepared as described by Dubowchik et. al.¹⁸ Conjugates containing DM4 linked to an antibody via the SPDB or sulfo-SPDB linkers were prepared as described previously with maytansinoid/antibody ratios (MAR) as follows, **1a** MAR = 4.0, **1b** MAR = 4.1, **1c** MAR = 3.9, **1d** MAR = 3.8, **1e** MAR = 3.9 each of the conjugates contained less than 2% aggregate and endotoxin units (EU) were below 0.2 EU/mg.²¹ Enzyme-linked immunosorbent assay (ELISA) methods for the determination of relative antibody and maytansinoid amounts in a given conjugate were performed as previously described.²⁶ Samples for HPLC/MS analysis of AaMC metabolites formed by incubating **8g** with COLO 205 cells were performed as described by Erickson et. al.¹

Preparative C18 HPLC method 1. Column 250 x 29 cm C18 packed in a load and lock system (available from Agilent); Flow rate 40 mL/min; Eluting with deionized water containing 0.2% formic acid with 5% acetonitrile for 5 min then a linear gradient from 5% - 95% acetonitrile for the next 30 min and maintaining 95% acetonitrile for 5 min with 220 nm and 252 nm detection. If required, particulates were removed from samples by centrifugation prior to purification.

HPLC analytical method 1. A HISEP 25 cm x 4.6 mm, 5 μm , Supelco column was eluted at room temperature, flow rate 0.7 mL/min with 100 mM ammonium acetate pH 7.0 buffer and a gradient of acetonitrile as follows: linear 25 – 40% 0 – 25 min; linear 40 – 100% 25 – 27 min. After which the column was maintained at 100% acetonitrile for 5 min then reequilibrated in starting conditions.

HPLC analytical method 2. A C8 150 x 2.1 mm 100, 5 μm , Kromasil column was eluted at room temperature, flow rate of 0.2 mL/min with deionized water containing 0.1% formic acid and with a gradient of acetonitrile as follows: linear 15 - 32% 0-15 min; linear 32 - 48% 15 – 25

1
2
3 min; linear 48 -58% 25 – 35 min; linear 58-90% 35-45 min; linear 90-15% 45 – 50 min with 9
4 min re-equilibration between runs. Detection by uv/vis 220 – 350 nm and by mass spectroscopy
5 in alternating positive and negative ion modes.
6
7

8 **Preparation of AaMC precursors and the AaMC metabolite PA-May 9.**

9
10 **4-Nitro-PA-May (20):** To a 57 mM solution of DM1 (211 mg, 0.286 mmol) in DMSO was
11 added 1-(bromomethyl)-4-nitrobenzene (74.1 mg, 0.343 mmol), then DBU (47.9 mg, 0.314
12 mmol) at room temperature. After 16 h the mixture was purified on an intelliflash system with a
13 100 g C18 cartridge, using deionized water with 0.1% formic acid and gradient of acetonitrile 30
14 % - 90% over 30 min, at a flow rate of 60 mL/min. The product fractions were combined, frozen
15 and lyophilized to give 109 mg, (47% yield) as an off-white solid. ¹H NMR (400 MHz,
16 Chloroform-d) δ 0.77 (s, 3H), 1.15 – 1.26 (m, 2H), 1.26 – 1.32 (m, 3H), 1.45 (td, J = 10.1, 5.4
17 Hz, 2H), 1.56 (s, 1H), 1.63 (s, 3H), 2.16 (dd, J = 14.5, 3.1 Hz, 2H), 2.43 – 2.78 (m, 6H), 2.81 (s,
18 3H), 2.96 – 3.04 (m, 2H), 3.16 (s, 3H), 3.35 (s, 3H), 3.44 – 3.54 (m, 2H), 3.74 (d, J = 3.1 Hz,
19 2H), 4.00 (s, 3H), 4.21 – 4.31 (m, 1H), 4.76 (dd, J = 12.0, 3.1 Hz, 1H), 5.34 (q, J = 6.8 Hz, 1H),
20 5.62 (dd, J = 15.3, 9.0 Hz, 1H), 6.20 (s, 1H), 6.35 – 6.46 (m, 1H), 6.55 (d, J = 1.7 Hz, 1H), 6.65
21 (d, J = 11.1 Hz, 1H), 6.78 (d, J = 1.8 Hz, 1H), 7.38 (d, J = 8.7 Hz, 2H), 8.08 (d, J = 8.7 Hz, 2H).
22 HRMS (M + H)⁺ calcd. 873.3142, found 873.3124.
23
24
25
26
27
28

29 **PA-May (9):** To a 0.05 M solution of 4-Nitro-PA-May (109 mg, 0.125 mmol) in 3:1
30 tetrahydrofuran:methanol (40 mL) was added a 5.5 M aqueous solution of ammonium chloride
31 (66.8 mg, 1.248 mmol) and powdered iron (34.8 mg, 0.624 mmol) at 50 °C. After 16 h the
32 reaction was cooled to room temperature, diluted with 10:1 tetrahydrofuran/methanol
33 (~equivalent volume) and vacuum filtered through Celite filter aid. The greenish-yellow filtrate
34 was rotary evaporated under vacuum. The yellow solid was redissolved in 4:1 acetonitrile:water
35 (20 mL) and purified on an intelliflash system with a 100 g flash C18 cartridge, using deionized
36 water with 0.1% formic acid and gradient of acetonitrile 20% - 95% over 30 min, at a flow rate
37 of 60 mL/min. The product fractions were frozen and lyophilized to give 32.5 mg (27% yield)
38 of desired product as a white solid. ¹H NMR (400 MHz, chloroform-d) δ 0.78 (s, 3H), 1.17 –
39 1.26 (m, 2H), 1.29 (d, J = 6.6 Hz, 3H), 1.40 – 1.51 (m, 2H), 1.52 – 1.60 (m, 1H), 1.63 (s, 6H),
40 2.16 (dd, J = 14.4, 3.1 Hz, 2H), 2.32 – 2.45 (m, 1H), 2.49-2.68 (m, 4H), 2.76 (s, 3H), 3.01 (d, J =
41 9.6 Hz, 1H), 3.08 (d, J = 12.6 Hz, 1H), 3.14 (s, 3H), 3.35 (s, 3H), 3.49 (d, J = 9.0 Hz, 1H), 3.57
42 (s, 2H), 3.62 (d, J = 12.7 Hz, 1H), 3.99 (s, 3H), 4.20 – 4.32 (m, 1H), 4.76 (dd, J = 12.0, 3.1 Hz,
43 1H), 5.35 (q, J = 6.8 Hz, 1H), 5.64 (dd, J = 15.3, 9.0 Hz, 1H), 6.24 (s, 1H), 6.42 (dd, J = 15.4,
44 11.1 Hz, 1H), 6.54 – 6.63 (m, 3H), 6.70 (d, J = 11.1 Hz, 1H), 6.82 (d, J = 1.8 Hz, 1H), 6.99 (d, J
45 = 8.2 Hz, 2H). HRMS (M + H)⁺ calcd. 843.3400, found 843.3388.
46
47
48
49
50
51
52

53 **General Procedure for the preparation of Fmoc protected dipeptides Fmoc-D-Ala-D-Ala-**
54 **OH (12b) and Fmoc-D-Ala-L-Ala-OH (12c).** Fmoc-D-Ala-OH (3.0 g, 9.6 mmol), *N*-
55 hydroxysuccinimide (6.4 g, 12.1 mmol) and EDC (1.8 g, 9.6 mmol) were taken up in
56 dichloromethane (50 mL) at room temperature. After 2 h the solution was washed with 0.25 M
57
58
59
60

HCl (2 x 50 mL) then with saturated aqueous sodium chloride (40 mL). The organic layer was dried over anhydrous sodium sulfate then vacuum filtered and solvent was removed from the filtrate under vacuum. Residue was taken up in 1,2-dimethoxyethane (45 mL) to which was added a solution of *L*-alanine or *D*-alanine (2.3 g, 25 mmol) in sodium bicarbonate (1.94 g, 23 mmol) dissolved in deionized water (45 mL) and dimethoxyethane (10 mL) followed after 2 min by addition of dimethoxyethane (35 mL). After 2 h the mixture was vacuum filtered and the filtrate was purified on a 450 g C18 cartridge eluting at 80 mL/min with deionized water containing 0.1% formic acid and a gradient of acetonitrile (5 to 95% over 35 min). Fractions containing desired compound were pooled, frozen and lyophilized.

Fmoc-*D*-Ala-*D*-Ala-OH (12b). White solid (41% yield). $^1\text{H NMR}$ (400 MHz, DMSO-*d*₆) δ 12.52 (s, 1H), 8.12 (d, $J = 7.3$ Hz, 1H), 7.89 (d, $J = 7.5$ Hz, 2H), 7.73 (t, $J = 7.2$ Hz, 2H), 7.49 (d, $J = 7.8$ Hz, 1H), 7.42 (td, $J = 7.5, 1.1$ Hz, 2H), 7.33 (td, $J = 7.5, 1.2$ Hz, 2H), 4.30 – 4.16 (m, 4H), 4.09 (q, $J = 7.3$ Hz, 1H), 1.27 (d, $J = 7.3$ Hz, 3H), 1.22 (d, $J = 7.1$ Hz, 3H). HRMS ($\text{M} + \text{Na}$)⁺ calcd. 405.1427, found 405.1417.

Fmoc-*D*-Ala-*L*-Ala-OH (12c). White solid (38 % yield). $^1\text{H NMR}$ (400 MHz, DMSO-*d*₆) δ 1.23 (d, $J = 7.3$ Hz, 3H), 1.26 (d, $J = 7.2$ Hz, 3H), 4.05 – 4.16 (m, 1H), 4.24 (dq, $J = 13.2, 7.2$ Hz, 4H), 7.33 (t, $J = 7.5$ Hz, 2H), 7.41 (t, $J = 7.4$ Hz, 2H), 7.47 (d, $J = 8.0$ Hz, 1H), 7.73 (t, $J = 7.2$ Hz, 2H), 7.88 (d, $J = 7.5$ Hz, 2H), 8.10 (d, $J = 7.4$ Hz, 1H). $^{13}\text{C NMR}$ (101 MHz, DMSO) δ 17.47, 18.54, 46.64, 47.47, 49.86, 65.64, 120.05, 125.27, 125.32, 127.05, 127.60, 140.68, 143.78, 143.89, 155.56, 172.13, 173.93. HRMS ($\text{M} + \text{Na}$)⁺ calcd. 405.1427, found 405.1411.

Fmoc-*L*-Ala-*D*-Ala-OH (12d). Fmoc-*L*-Ala-ONHS (3.0 g, 7.35 mmol) was taken up in 1,2-dimethoxyethane (45 mL) to which was added a solution of H-*D*-Ala-OH (2.5 g, 26 mmol) in sodium bicarbonate (2.0 g, 23.2 mmol) dissolved in deionized water (47 mL) and dimethoxyethane (11 mL) followed after 2 min by adding dimethoxyethane (37 mL). After 2 h the mixture was vacuum filtered and the filtrate was purified on a 450 g C18 cartridge eluting at 80 mL/min with deionized water and an acetonitrile gradient of acetonitrile (5 to 95% over 35 min). Fractions containing desired compound were pooled, frozen and lyophilized to give 1.3 g, (46 % yield) of product as a white solid. $^1\text{H NMR}$ (400 MHz, DMSO-*d*₆) δ 1.24 (d, $J = 7.2$ Hz, 3H), 1.27 (d, $J = 7.3$ Hz, 3H), 4.14 (t, $J = 7.5$ Hz, 1H), 4.19 – 4.35 (m, 3H), 7.32 (t, $J = 7.5$ Hz, 2H), 7.41 (t, $J = 7.5$ Hz, 2H), 7.48 (d, $J = 8.1$ Hz, 1H), 7.74 (t, $J = 7.5$ Hz, 2H), 7.87 (d, $J = 7.5$ Hz, 2H), 8.13 (t, $J = 8.2$ Hz, 1H), 11.97 – 13.16 (m, 1H). $^{13}\text{C NMR}$ (101 MHz, DMSO) δ 174.02, 172.25, 155.64, 143.95, 143.83, 140.75, 127.67, 127.11, 125.39, 125.34, 120.12, 65.71, 49.93, 47.53, 46.70, 18.62, 17.51. HRMS ($\text{M} + \text{Na}$)⁺ calcd. 405.1427, found 405.1409.

General Procedure for the preparation of 13b – 13f. To a 20 mL capacity flask was added 4-amino-benzylalcohol (0.25 g, 3.0 mmol), one of the Fmoc protected dipeptides (**12b-12d**) or Fmoc-Gly-Gly-OH (0.65 mmol), and EEDQ (0.32 g, 1.3 mmol) followed by 2:1 dichloromethane:methanol (10 mL). After 16 h, solvent was evaporated under vacuum and residue was vigorously triturated with diethyl ether (40 mL). The suspension was vacuum

1
2
3 filtered while continuously scrapping the filter paper. The filter cake was washed with diethyl
4 ether (10 mL) and dried under vacuum.
5
6

7 **Fmoc-D-Ala-D-Ala-PAB-OH (13b).** White solid (56 % yield). ^1H NMR (400 MHz, DMSO-
8 d_6) δ 1.24 (d, $J = 7.0$ Hz, 3H), 1.31 (d, $J = 7.0$ Hz, 3H), 4.11 (q, $J = 7.1$ Hz, 1H), 4.19 – 4.33 (m,
9 3H), 4.36 – 4.51 (m, 4H), 5.10 (t, $J = 5.6$ Hz, 1H), 7.23 (d, $J = 8.1$ Hz, 2H), 7.33 (t, $J = 7.4$ Hz,
10 2H), 7.42 (t, $J = 7.4$ Hz, 2H), 7.55 (dd, $J = 7.8, 4.9$ Hz, 3H), 7.72 (t, $J = 8.1$ Hz, 2H), 7.89 (d, $J =$
11 7.5 Hz, 2H), 8.10 (d, $J = 7.2$ Hz, 1H), 9.88 (s, 1H). HRMS (M + Na) $^+$ calcd. 510.2005, found
12 510.1985.
13
14

15
16 **Fmoc-D-Ala-L-Ala-PAB-OH (13c).** White solid (64 % yield). ^1H NMR (400 MHz, DMSO- d_6)
17 δ 1.27 (d, $J = 7.1$ Hz, 3H), 1.34 (d, $J = 7.0$ Hz, 3H), 4.14 (t, $J = 7.0$ Hz, 1H), 4.22 (t, $J = 6.9$ Hz,
18 1H), 4.31 (d, $J = 6.2$ Hz, 2H), 4.46 (q, $J = 4.4, 3.2$ Hz, 3H), 5.14 (d, $J = 5.4$ Hz, 1H), 7.25 (d, $J =$
19 8.3 Hz, 2H), 7.33 (t, $J = 7.4$ Hz, 2H), 7.40 (td, $J = 7.4, 4.6$ Hz, 2H), 7.62 (d, $J = 8.3$ Hz, 2H), 7.64
20 – 7.77 (m, 3H), 7.87 (dd, $J = 7.5, 2.8$ Hz, 2H), 8.33 (d, $J = 7.5$ Hz, 1H), 9.75 (s, 1H). ^{13}C NMR
21 (101 MHz, DMSO) δ 172.53, 70.86, 156.00, 143.87, 143.74, 140.74, 137.64, 137.40, 127.65,
22 127.09, 126.89, 125.29, 125.24, 120.10, 119.12, 65.77, 62.65, 50.25, 48.95, 46.68, 18.17, 17.93.
23 HRMS (M + Na) $^+$ calcd. 510.2005, found 510.1987.
24
25
26

27
28 **Fmoc-L-Ala-D-Ala-PAB-OH (13d).** White solid (48 % yield). ^1H NMR (400 MHz, DMSO- d_6)
29 δ 1.26 (d, $J = 7.0$ Hz, 3H), 1.32 (d, $J = 7.0$ Hz, 3H), 4.13 (p, $J = 7.3$ Hz, 1H), 4.22 (q, $J = 6.7, 4.7$
30 Hz, 1H), 4.30 (d, $J = 6.2$ Hz, 2H), 4.45 (d, $J = 5.0$ Hz, 3H), 5.13 (t, $J = 5.7$ Hz, 1H), 7.24 (d, $J =$
31 8.2 Hz, 2H), 7.32 (t, $J = 7.4$ Hz, 2H), 7.40 (td, $J = 7.5, 4.9$ Hz, 2H), 7.60 (d, $J = 7.9$ Hz, 2H), 7.63
32 – 7.75 (m, 3H), 7.87 (dd, $J = 7.5, 3.0$ Hz, 2H), 8.31 (d, $J = 7.6$ Hz, 1H), 9.73 (s, 1H). HRMS (M
33 + Na) $^+$ calcd. 510.2005, found 510.1986.
34
35

36 **Fmoc-L-Ala-L-Ala-PAB-OH (13e).** White solid (75 % yield). ^1H NMR (400 MHz, DMSO- d_6)
37 δ 1.24 (d, $J = 7.1$ Hz, 3H), 1.31 (d, $J = 7.0$ Hz, 3H), 4.11 (q, $J = 7.1$ Hz, 1H), 4.17 – 4.32 (m,
38 3H), 4.42 (dd, $J = 11.9, 6.3$ Hz, 3H), 5.10 (t, $J = 5.7$ Hz, 1H), 7.24 (d, $J = 8.3$ Hz, 2H), 7.33 (t, J
39 = 7.4 Hz, 2H), 7.41 (t, $J = 7.5$ Hz, 2H), 7.55 (dd, $J = 7.7, 4.2$ Hz, 3H), 7.72 (t, $J = 8.2$ Hz, 2H),
40 7.89 (d, $J = 7.5$ Hz, 2H), 8.11 (d, $J = 7.3$ Hz, 1H), 9.88 (s, 1H). ^{13}C NMR (101 MHz, DMSO) δ
41 171.02, 170.57, 170.53, 168.09, 155.24, 151.21, 143.85, 143.75, 141.25, 141.23, 140.68, 139.39,
42 138.30, 137.59, 133.23, 132.56, 128.93, 128.89, 128.45, 127.60, 127.25, 127.05, 125.25, 125.13,
43 121.35, 120.07, 119.99, 119.02, 117.11, 113.90, 109.69, 88.19, 79.97, 78.62, 77.62, 73.14, 66.74,
44 59.99, 56.53, 56.09, 51.64, 49.99, 49.96, 48.96, 46.64, 45.40, 37.68, 36.33, 35.16, 34.86, 33.32,
45 31.91, 29.68, 25.97, 18.14, 15.01, 14.39, 13.04, 11.35. HRMS (M + Na) $^+$ calcd. 510.2005, found
46 510.1989.
47
48
49
50

51
52 **Fmoc-Gly-Gly-PAB-OH (13f).** White solid (56 % yield). ^1H NMR (400 MHz, DMSO- d_6) δ
53 3.71 (d, $J = 6.0$ Hz, 2H), 3.92 (d, $J = 5.8$ Hz, 2H), 4.24 (t, $J = 7.0$ Hz, 1H), 4.32 (d, $J = 7.1$ Hz,
54 2H), 4.44 (s, 2H), 5.11 (s, 1H), 7.25 (d, $J = 8.5$ Hz, 2H), 7.33 (t, $J = 7.4$ Hz, 2H), 7.41 (t, $J = 7.5$
55 Hz, 2H), 7.56 (d, $J = 8.1$ Hz, 2H), 7.66 (t, $J = 6.1$ Hz, 1H), 7.72 (d, $J = 7.5$ Hz, 2H), 7.88 (d, $J =$
56 7.5 Hz, 2H), 8.25 (q, $J = 8.5, 5.9$ Hz, 1H), 9.82 (s, 1H). ^{13}C NMR (101 MHz, DMSO) δ 40.88,
57
58
59
60

41.80, 44.86, 60.83, 64.01, 117.14, 118.28, 123.43, 125.14, 125.27, 125.82, 135.56, 135.68, 138.92, 142.02, 154.83, 165.62, 167.77. HRMS (M + Na)⁺ calcd. 510.2005, found 510.1992.

General Procedure for the preparation of compounds (14a – 14f). To a solution of one of the compounds **13a – 13f** (0.24 mmol) in anhydrous DMF (700 μ L) dichloromethane was added DIPEA (56 μ L, 0.32 mmol) and methanesulfonyl chloride (20 μ L, 0.26 mmol). After 1 h sodium bromide (0.82 mg, 0.80 mmol) was added then after 90 min 1:1 dichloromethane:DMF (2 mL) was added and the mixture was centrifuged in a speedvac for 5 min without vacuum. The supernatant was transferred to a 10 mL flask to which was added DM1 (118 mg, 0.16 mmol). After 45 min the sample was purified by preparative HPLC method 1. Fractions containing pure desired product were combined in a 200 mL flask, frozen in a dry ice acetone bath then lyophilized.

Fmoc-L-Val-L-Cit-PA-May (14a). White solid (32 % yield). ¹H NMR (400 MHz, CDCl₃) 0.81 (s, 3H), 0.98 – 0.86 (m, 6H), 1.19 (d, *J* = 6.1 Hz, 3H), 1.23 (d, *J* = 6.6 Hz, 3H), 1.56 – 1.29 (m, 5H), 1.63 (s, 3H), 1.84 – 1.72 (m, 1H), 2.12 – 1.98 (m, 2H), 2.44 (dd, *J* = 14.9, 7.4 Hz, 1H), 2.57 – 2.50 (m, 3H), 2.59 (s, 2H), 2.70 – 2.63 (m, 1H), 2.73 (s, 3H), 2.85 (d, *J* = 9.5 Hz, 1H), 3.07 – 2.95 (m, 1H), 3.17-3.08(m, 5H), 3.31 (s, 3H), 3.54 – 3.34 (m, 4H), 3.67 – 3.55 (m, 2H), 3.97 (s, 3H), 4.01 (d, *J* = 6.7 Hz, 1H), 4.14 (t, *J* = 11.4 Hz, 1H), 4.32 – 4.21 (m, 2H), 4.41 – 4.32 (m, 1H), 4.63 – 4.45 (m, 2H), 5.46 – 5.33 (m, 2H), 5.63 (dd, *J* = 14.9, 9.1 Hz, 1H), 6.09 – 5.90 (m, 1H), 6.68 – 6.47 (m, 3H), 6.80 (s, 1H), 7.14 – 7.07 (m, 2H), 7.38-7.30 (m, 3H), 7.46 – 7.38 (m, 2H), 7.53 (d, *J* = 8.1 Hz, 2H), 7.74 (t, *J* = 7.4 Hz, 2H), 7.86 (d, *J* = 7.4 Hz, 2H), 8.10 (d, *J* = 7.4 Hz, 1H), δ 10.00 (s, 1H). HRMS (M + Na)⁺ calcd. 1343.5441; Found 1343.5378

Fmoc-D-Ala-D-Ala-PA-May (14b). White solid (41 % yield). ¹H NMR (400 MHz, DMSO-d₆) δ 0.76 (s, 3H), 1.12 (d, *J* = 6.3 Hz, 3H), 1.16 (d, *J* = 6.8 Hz, 3H), 1.21 – 1.26 (m, 6H), 1.31 (dd, *J* = 7.3, 3.0 Hz, 5H), 1.44 (dd, *J* = 15.3, 9.9 Hz, 2H), 1.57 (s, 3H), 2.03 (dd, *J* = 14.7, 2.4 Hz, 1H), 2.37 (ddd, *J* = 16.0, 7.6, 3.5 Hz, 1H), 2.67 (s, 3H), 2.78 (d, *J* = 9.7 Hz, 1H), 3.07 (s, 3H), 3.13 (d, *J* = 12.5 Hz, 1H), 3.24 (s, 3H), 3.37 (d, *J* = 12.4 Hz, 1H), 3.47 (d, *J* = 9.0 Hz, 1H), 3.55 – 3.66 (m, 2H), 3.93 (s, 3H), 4.02 – 4.14 (m, 3H), 4.19 – 4.30 (m, 4H), 4.42 (d, *J* = 9.4 Hz, 3H), 4.52 (dd, *J* = 11.9, 2.8 Hz, 1H), 5.30 (q, *J* = 6.7 Hz, 1H), 5.56 (dd, *J* = 13.7, 9.0 Hz, 1H), 6.49 – 6.60 (m, 3H), 6.87 (s, 1H), 7.09 (d, *J* = 8.2 Hz, 2H), 7.15 (d, *J* = 1.8 Hz, 1H), 7.23 (d, *J* = 8.2 Hz, 1H), 7.33 (t, *J* = 7.5 Hz, 3H), 7.41 (t, *J* = 7.6 Hz, 2H), 7.46 (d, *J* = 8.2 Hz, 2H), 7.54 (dd, *J* = 8.0, 2.9 Hz, 3H), 7.72 (t, *J* = 8.1 Hz, 2H), 7.89 (d, *J* = 7.6 Hz, 2H), 8.10 (t, *J* = 6.4 Hz, 1H), 9.89 (d, *J* = 11.6 Hz, 1H). HRMS (M + Na)⁺ calcd 1229.4649, 1229.4584.

Fmoc-D-Ala-L-Ala-PA-May (14c). White solid (35 % yield). ¹H NMR (400 MHz, DMSO-d₆) δ 0.72 (d, *J* = 6.5 Hz, 3H), 1.12 (d, *J* = 6.3 Hz, 3H), 1.15 (d, *J* = 6.8 Hz, 3H), 1.24 (dd, *J* = 7.0, 3.7 Hz, 3H), 1.29 – 1.33 (m, 3H), 1.38 – 1.46 (m, 2H), 1.56 (d, *J* = 2.5 Hz, 3H), 2.02 (d, *J* = 14.5 Hz, 1H), 2.32 – 2.41 (m, 1H), 2.59 – 2.64 (m, 1H), 2.67 (s, 3H), 2.78 (d, *J* = 9.6 Hz, 1H), 3.06 (d, *J* = 1.4 Hz, 2H), 3.11 (s, 1H), 3.19 (s, 1H), 3.24 (s, 1H), 3.32 (s, 5H), 3.43 (dd, *J* = 12.3, 9.1 Hz, 1H), 3.55 – 3.64 (m, 2H), 3.93 (s, 3H), 4.02 – 4.14 (m, 2H), 4.21 (t, *J* = 6.2 Hz, 1H), 4.24 – 4.29 (m, 2H), 4.42 (t, *J* = 6.8 Hz, 1H), 4.51 (dd, *J* = 11.9, 2.5 Hz, 1H), 5.29 (q, *J* = 6.7 Hz, 1H), 5.54

(ddd, $J = 13.7, 8.9, 3.9$ Hz, 1H), 5.91 (s, 1H), 6.45 – 6.52 (m, 2H), 6.56 (d, $J = 11.1$ Hz, 1H), 6.86 (d, $J = 10.8$ Hz, 1H), 7.07 (dd, $J = 8.3, 2.6$ Hz, 2H), 7.14 (dd, $J = 8.1, 1.7$ Hz, 1H), 7.32 (td, $J = 7.5, 5.7, 3.9$ Hz, 3H), 7.39 (q, $J = 7.1$ Hz, 3H), 7.49 (dd, $J = 8.3, 5.3$ Hz, 2H), 7.62 (d, $J = 6.9$ Hz, 1H), 7.70 (td, $J = 12.1, 10.2, 5.1$ Hz, 2H), 7.87 (dd, $J = 7.5, 3.5$ Hz, 2H), 8.27 – 8.32 (m, 1H), 9.75 (d, $J = 11.1$ Hz, 1H). ^{13}C NMR (101 MHz, DMSO) δ 172.48, 172.43, 171.09, 170.89, 170.53, 168.08, 155.87, 155.22, 151.21, 143.84, 143.79, 143.71, 143.64, 141.23, 140.67, 138.34, 137.42, 133.35, 132.54, 129.40, 128.89, 128.85, 128.42, 127.61, 127.05, 125.26, 125.20, 121.53, 120.08, 119.15, 117.08, 113.91, 88.16, 82.95, 79.95, 77.60, 73.13, 66.72, 65.69, 59.98, 56.53, 56.08, 51.62, 50.10, 48.89, 46.60, 45.38, 37.67, 36.33, 35.15, 34.84, 33.27, 31.89, 29.66, 25.95, 18.12, 18.02, 14.99, 14.39, 13.04, 11.32. HRMS ($\text{M} + \text{Na}$) $^{+}$ 1229.4649, found 1229.4615.

Fmoc-L-Ala-D-Ala-PA-May (14d). White solid (33 % yield). ^1H NMR (400 MHz, DMSO- d_6) δ 0.76 (s, 3H), 1.12 (d, $J = 6.5$ Hz, 3H), 1.16 (d, $J = 6.8$ Hz, 3H), 1.24 (d, $J = 7.2$ Hz, 3H), 1.31 (dd, $J = 6.8, 2.4$ Hz, 3H), 1.40 – 1.49 (m, 2H), 1.58 (s, 3H), 2.03 (dd, $J = 14.5, 2.8$ Hz, 1H), 2.37 (ddd, $J = 16.3, 8.2, 5.8$ Hz, 1H), 2.59 – 2.65 (m, 1H), 2.67 (s, 3H), 2.69 - 2.76 (m, 1H), 2.78 (d, $J = 9.7$ Hz, 1H), 3.07 (s, 3H), 3.13 (d, $J = 12.7$ Hz, 1H), 3.24 (d, $J = 3.1$ Hz, 3H), 3.47 (dd, $J = 9.0, 3.1$ Hz, 1H), 3.55 – 3.65 (m, 2H), 3.93 (d, $J = 2.4$ Hz, 3H), 4.03 – 4.12 (m, 2H), 4.22 (d, $J = 6.8$ Hz, 1H), 4.27 (d, $J = 8.1$ Hz, 1H), 4.41 (q, $J = 7.1, 6.6$ Hz, 1H), 4.52 (dd, $J = 11.9, 2.8$ Hz, 1H), 5.30 (q, $J = 6.8$ Hz, 1H), 5.55 (dd, $J = 13.6, 9.1$ Hz, 1H), 5.93 (s, 1H), 6.49 – 6.59 (m, 3H), 6.87 (s, 1H), 7.07 – 7.12 (m, 2H), 7.15 (d, $J = 1.8$ Hz, 1H), 7.30 – 7.37 (m, 2H), 7.41 (t, $J = 7.5$ Hz, 2H), 7.47 (dd, $J = 8.5, 2.7$ Hz, 2H), 7.55 (d, $J = 7.5$ Hz, 1H), 7.72 (t, $J = 8.1$ Hz, 2H), 7.84 (d, $J = 7.4$ Hz, 1H), 7.88 (d, $J = 7.5$ Hz, 2H), 8.14 (d, $J = 7.2$ Hz, 1H), 9.94 (s, 1H). ^{13}C NMR (101 MHz, DMSO) δ 172.47, 170.89, 170.52, 168.06, 155.22, 151.21, 143.82, 143.63, 141.25, 141.20, 140.66, 138.38, 133.29, 132.51, 128.86, 127.59, 127.03, 125.26, 125.19, 121.50, 120.04, 119.15, 117.08, 113.86, 88.17, 79.94, 77.61, 77.57, 73.12, 66.71, 65.72, 59.95, 56.51, 56.00, 51.60, 50.12, 48.98, 46.60, 37.67, 36.32, 35.13, 34.85, 33.26, 31.87, 29.64, 25.90, 18.07, 17.99, 14.98, 14.39, 13.03, 11.33. HRMS ($\text{M} + \text{Na}$) $^{+}$ 1229.4649, found 1229.4622.

Fmoc-L-Ala-L-Ala-PA-May (14e). White solid (43% yield). ^1H NMR (400 MHz, DMSO- d_6) δ 0.76 (s, 3H), 1.12 (d, $J = 6.5$ Hz, 3H), 1.16 (d, $J = 6.8$ Hz, 3H), 1.24 (d, $J = 7.2$ Hz, 3H), 1.31 (dd, $J = 6.8, 2.4$ Hz, 3H), 1.40 – 1.49 (m, 2H), 1.58 (s, 3H), 2.03 (dd, $J = 14.5, 2.8$ Hz, 1H), 2.37 (ddd, $J = 16.3, 8.2, 5.8$ Hz, 1H), 2.59 – 2.65 (m, 1H), 2.67 (s, 3H), 2.69 - 2.76 (m, 1H), 2.78 (d, $J = 9.7$ Hz, 1H), 3.07 (s, 3H), 3.13 (d, $J = 12.7$ Hz, 1H), 3.24 (d, $J = 3.1$ Hz, 3H), 3.47 (dd, $J = 9.0, 3.1$ Hz, 1H), 3.55 – 3.65 (m, 2H), 3.93 (d, $J = 2.4$ Hz, 3H), 4.03 – 4.12 (m, 2H), 4.22 (d, $J = 6.8$ Hz, 1H), 4.27 (d, $J = 8.1$ Hz, 1H), 4.41 (q, $J = 7.1, 6.6$ Hz, 1H), 4.52 (dd, $J = 11.9, 2.8$ Hz, 1H), 5.30 (q, $J = 6.8$ Hz, 1H), 5.55 (dd, $J = 13.6, 9.1$ Hz, 1H), 5.93 (s, 1H), 6.49 – 6.59 (m, 3H), 6.87 (s, 1H), 7.07 – 7.12 (m, 2H), 7.15 (d, $J = 1.8$ Hz, 1H), 7.30 – 7.37 (m, 2H), 7.41 (t, $J = 7.5$ Hz, 2H), 7.47 (dd, $J = 8.5, 2.7$ Hz, 2H), 7.55 (d, $J = 7.5$ Hz, 1H), 7.72 (t, $J = 8.1$ Hz, 2H), 7.84 (d, $J = 7.4$ Hz, 1H), 7.88 (d, $J = 7.5$ Hz, 2H), 8.14 (d, $J = 7.2$ Hz, 1H), 9.94 (s, 1H). HRMS ($\text{M} + \text{Na}$) $^{+}$ 1229.4649, found 1229.4614.

Fmoc-Gly-Gly-PA-May (14f). White solid (38 % yield). ^1H NMR (400 MHz, $\text{DMSO-}d_6$) δ 0.74 (s, 3H), 1.12 (d, $J = 6.3$ Hz, 3H), 1.16 (d, $J = 6.8$ Hz, 3H), 1.23 (d, $J = 13.0$ Hz, 2H), 1.43 (dd, $J = 14.3, 7.7$ Hz, 2H), 1.58 (s, 3H), 2.06 (dd, $J = 20.2, 8.5$ Hz, 1H), 2.30 – 2.45 (m, 1H), 2.69 (d, $J = 7.9$ Hz, 5H), 2.79 (d, $J = 9.7$ Hz, 2H), 3.00 – 3.18 (m, 4H), 3.25 (d, $J = 10.5$ Hz, 4H), 3.61 (q, $J = 13.5$ Hz, 2H), 3.70 (d, $J = 5.8$ Hz, 2H), 3.83 – 4.04 (m, 5H), 4.07 (t, $J = 11.4$ Hz, 1H), 4.25 (d, $J = 6.5$ Hz, 1H), 4.30 (d, $J = 7.0$ Hz, 2H), 4.40 – 4.62 (m, 1H), 5.30 (q, $J = 6.8$ Hz, 1H), 5.55 (dd, $J = 14.2, 9.2$ Hz, 1H), 5.93 (s, 1H), 6.42 – 6.68 (m, 3H), 6.82 – 6.95 (m, 1H), 7.04 – 7.20 (m, 3H), 7.32 (dd, $J = 14.9, 7.5$ Hz, 2H), 7.38 – 7.52 (m, 4H), 7.65 (t, $J = 5.8$ Hz, 1H), 7.72 (d, $J = 7.4$ Hz, 2H), 7.89 (d, $J = 7.5$ Hz, 2H), 8.15 – 8.37 (m, 1H). ^{13}C NMR (101 MHz, DMSO) δ 11.34, 13.05, 14.40, 15.01, 25.98, 29.68, 31.91, 33.31, 34.85, 35.16, 36.34, 37.68, 42.67, 43.54, 45.39, 46.63, 51.63, 56.08, 56.54, 59.99, 65.80, 66.74, 73.15, 77.61, 79.97, 88.18, 113.91, 117.10, 119.04, 120.09, 121.56, 125.09, 125.23, 127.07, 127.62, 128.42, 128.94, 132.58, 133.27, 137.41, 138.39, 140.70, 141.25, 143.81, 151.23, 155.24, 156.61, 167.47, 168.10, 169.57, 170.54, 170.57. HRMS ($\text{M} + \text{Na}$) $^+$ calcd. 1229.4649, found 1229.4584.

General Procedure for the preparation of compounds (15a – 15f). One of the compounds (14a – 14f) (0.10 mmol) was dissolved in anhydrous DMF (2 mL) to which excess morpholine (250 μL) was added. After 45 min the reaction was purified by preparative HPLC method 1. Fractions containing the desired product were combined in a 200 mL flask, frozen in a dry ice acetone bath then lyophilized.

$\text{H}_2\text{N-L-Val-L-Cit-PA-May}$ (15a). Thick colorless oil (72% yield). ^1H NMR (400 MHz, $\text{DMSO-}d_6$) δ 0.76 (s, 3H), 0.95 (s, 3H), 0.97 (s, 3H), 1.14 (d, $J = 6.3$ Hz, 3H), 1.18 (d, $J = 6.8$ Hz, 3H), 1.24 – 1.55 (m, 5H), 1.58 (s, 3H), 1.60 – 1.71 (m, 1H), 1.71 – 1.84 (m, 1H), 1.99 (d, $J = 11.8$ Hz, 1H), 2.05 – 2.18 (m, 1H), 2.30 – 2.43 (m, 1H), 2.58 – 2.66 (m, 1H), 2.67 (s, 3H), 2.80 (d, $J = 9.6$ Hz, 1H), 2.96 – 3.06 (m, 1H), 3.07 (s, 3H), 3.27 (s, 3H), 3.36 – 3.78 (m, 2H), 3.93 (s, 3H), 4.05 – 4.16 (m, 1H), 4.49 – 4.64 (m, 2H), 5.32 (dd, $J = 13.4, 6.6$ Hz, 1H), 5.58 (dd, $J = 15.0, 9.1$ Hz, 1H), 6.43 – 6.63 (m, 3H), 6.71 (s, 1H), 7.06 (d, $J = 8.1$ Hz, 2H), 7.49 (d, $J = 8.5$ Hz, 2H), 8.07 – 8.18 (m, 2H), 8.69 (d, $J = 7.8$ Hz, 1H), 10.10 (s, 1H). HRMS ($\text{M} + \text{Na}$) $^+$ calcd. 1121.4761; found 1121.4717.

$\text{H}_2\text{N-D-Ala-D-Ala-PA-May}$ (15b). Thick colorless oil (76 % yield). ^1H NMR (400 MHz, $\text{DMSO-}d_6$) δ 0.77 (s, 3H), 1.12 (d, $J = 6.3$ Hz, 3H), 1.16 (d, $J = 6.8$ Hz, 6H), 1.24 (d, $J = 13.1$ Hz, 1H), 1.31 (d, $J = 6.9$ Hz, 3H), 1.45 (tt, $J = 10.1, 2.6$ Hz, 2H), 1.58 (s, 3H), 2.03 (dd, $J = 14.5, 2.9$ Hz, 1H), 2.31 – 2.42 (m, 2H), 2.55 – 2.65 (m, 3H), 2.67 (s, 3H), 2.69 – 2.76 (m, 1H), 2.78 (d, $J = 9.7$ Hz, 1H), 3.07 (s, 3H), 3.13 (d, $J = 12.5$ Hz, 1H), 3.25 (s, 3H), 3.34 – 3.37 (m, 2H), 3.48 (d, $J = 9.1$ Hz, 1H), 3.55 – 3.65 (m, 2H), 3.69 (t, $J = 4.6$ Hz, 1H), 3.94 (s, 3H), 4.02 – 4.10 (m, 1H), 4.39 – 4.48 (m, 1H), 4.52 (dd, $J = 12.0, 2.8$ Hz, 1H), 5.30 (q, $J = 6.8$ Hz, 1H), 5.51 – 5.59 (m, 1H), 5.92 (s, 1H), 6.49 – 6.54 (m, 2H), 6.56 (s, 1H), 6.88 (s, 1H), 7.08 – 7.13 (m, 2H), 7.16 (d, $J = 1.8$ Hz, 1H), 7.27 – 7.42 (m, 1H), 7.43 – 7.49 (m, 2H), 7.70 (d, $J = 7.4$ Hz, 0.5H), 7.86 (d, $J = 7.6$ Hz, 0.5H), 8.19 (s, 1H), 10.02 (s, 1H). HRMS ($\text{M} + \text{Na}$) $^+$ calcd. 1007.3962, found 1007.3958.

$\text{H}_2\text{N-D-Ala-L-Ala-PA-May}$ (15c). Thick colorless oil (84 % yield). ^1H NMR (400 MHz, $\text{DMSO-}d_6$) δ 0.76 (s, 3H), 1.06 – 1.24 (m, 7H), 1.24 – 1.49 (m, 5H), 1.58 (s, 3H), 1.99 (d, $J =$

1
2
3
4
5
6
7
8
9
10
11
12
13
14
15
16
17
18
19
20
21
22
23
24
25
26
27
28
29
30
31
32
33
34
35
36
37
38
39
40
41
42
43
44
45
46
47
48
49
50
51
52
53
54
55
56
57
58
59
60

14.2 Hz, 1H), 2.36 (dd, $J = 18.3, 9.7$ Hz, 1H), 2.58 – 2.74 (m, 4H), 2.80 (dd, $J = 9.6, 4.3$ Hz, 1H), 3.07 (d, $J = 3.4$ Hz, 3H), 3.27 (d, $J = 4.6$ Hz, 4H), 3.50 – 3.67 (m, 3H), 3.94 (d, $J = 3.9$ Hz, 3H), 4.09 (t, $J = 11.1$ Hz, 1H), 4.45 (d, $J = 7.1$ Hz, 1H), 4.49 – 4.62 (m, 1H), 5.33 (t, $J = 6.7$ Hz, 1H), 5.57 (dd, $J = 14.9, 8.9$ Hz, 1H), 5.90 (s, 1H), 6.34 – 6.67 (m, 3H), 6.66 – 6.78 (m, 1H), 7.07 (d, $J = 8.0$ Hz, 2H), 7.46 (dt, $J = 8.5, 2.8$ Hz, 2H), 8.28 (d, $J = 37.9$ Hz, 2H), 9.95 (d, $J = 6.9$ Hz, 1H). HRMS (M + H)⁺ calcd. 985.4148, found 985.4134.

H₂N-*L*-Ala-*D*-Ala-PA-May (15d). Thick colorless oil (75 % yield). ¹H NMR (400 MHz, DMSO-*d*₆) δ 0.76 (s, 3H), 1.12 (d, $J = 6.3$ Hz, 3H), 1.16 (d, $J = 6.8$ Hz, 3H), 1.21 (d, $J = 6.9$ Hz, 3H), 1.32 (d, $J = 7.0$ Hz, 3H), 1.38 – 1.50 (m, 2H), 1.58 (s, 3H), 2.03 (dd, $J = 14.4, 2.9$ Hz, 1H), 2.38 (ddd, $J = 16.0, 8.1, 5.9$ Hz, 1H), 2.54 (d, $J = 2.4$ Hz, 1H), 2.58 – 2.8 (m, 1H), 2.67 (s, 3H), 2.79 (d, $J = 9.6$ Hz, 1H), 3.07 (s, 3H), 3.14 (d, $J = 12.3$ Hz, 1H), 3.25 (s, 3H), 3.38 (d, $J = 12.4$ Hz, 1H), 3.48 (d, $J = 8.9$ Hz, 1H), 3.48 – 3.60 (m, 2H), 3.60 (d, $J = 7.5$ Hz, 1H), 3.94 (s, 3H), 4.01 – 4.12 (m, 1H), 4.13-4.38 (m, 2H), 4.43 (d, $J = 6.4$ Hz, 1H), 4.52 (dd, $J = 11.9, 2.8$ Hz, 1H), 5.30 (q, $J = 6.7$ Hz, 1H), 5.56 (dd, $J = 13.5, 9.2$ Hz, 1H), 6.48 – 6.61 (m, 3H), 6.89 (s, 1H), 7.10 (d, $J = 8.4$ Hz, 2H), 7.16 (d, $J = 1.9$ Hz, 1H), 7.49 (dd, $J = 8.6, 2.5$ Hz, 2H), 8.43 (s, 1H), 8.45 – 8.55 (m, 1H), 10.14 (s, 1H). ¹³C NMR (101 MHz, DMSO) δ 173.48, 171.02, 170.58, 170.55, 168.11, 155.27, 151.27, 141.26, 138.32, 137.57, 133.33, 132.58, 128.91, 128.47, 125.15, 121.59, 119.24, 117.14, 113.90, 88.22, 79.99, 77.63, 73.17, 66.77, 66.27, 60.00, 56.55, 56.11, 51.66, 49.39, 48.96, 45.44, 44.99, 37.71, 36.36, 35.17, 34.88, 33.36, 31.92, 29.70, 25.97, 20.05, 18.48, 15.03, 14.40, 13.06, 11.38. HRMS (M + H)⁺ calcd. 985.4148, found 985.4131.

H₂N-*L*-Ala-*L*-Ala-PA-May (15e). Thick colorless oil (81% yield). ¹H NMR (400 MHz, DMSO-*d*₆) δ 0.77 (s, 3H), 1.12 (d, $J = 6.3$ Hz, 3H), 1.16 (d, $J = 6.8$ Hz, 3H), 1.24 (d, $J = 12.2$ Hz, 1H), 1.28 (d, $J = 6.9$ Hz, 3H), 1.33 (d, $J = 7.0$ Hz, 3H), 1.40 – 1.50 (m, 2H), 1.58 (s, 3H), 2.03 (dd, $J = 14.5, 2.8$ Hz, 1H), 2.37 (ddd, $J = 16.1, 8.1, 5.8$ Hz, 1H), 2.54 (d, $J = 2.3$ Hz, 1H), 2.62 (dd, $J = 13.8, 6.1$ Hz, 1H), 2.67 (s, 3H), 2.68 – 2.75 (m, 1H), 2.78 (d, $J = 9.8$ Hz, 1H), 2.86 (t, $J = 4.8$ Hz, 0H), 3.06 (s, 3H), 3.14 (d, $J = 12.6$ Hz, 1H), 3.25 (s, 3H), 3.39 (d, $J = 12.5$ Hz, 1H), 3.48 (d, $J = 9.1$ Hz, 1H), 3.60 (d, $J = 7.6$ Hz, 2H), 3.63 – 3.71 (m, 1H), 3.93 (s, 3H), 4.02 – 4.10 (m, 1H), 4.45 (t, $J = 6.5$ Hz, 1H), 4.51 (dd, $J = 12.1, 2.8$ Hz, 1H), 5.30 (q, $J = 6.8$ Hz, 1H), 5.51 – 5.59 (m, 1H), 6.50 – 6.59 (m, 3H), 6.88 (s, 1H), 7.10 (d, $J = 8.4$ Hz, 2H), 7.16 (d, $J = 1.8$ Hz, 1H), 7.46 – 7.50 (m, 2H), 8.29 (s, 2H), 8.62 (d, $J = 7.3$ Hz, 1H), 10.13 (s, 1H). HRMS (M + Na)⁺ calcd. 985.4148, found 985.4137.

H₂N-Gly-Gly-PA-May (15f). Thick colorless oil (80 % yield). ¹H NMR (400 MHz, DMSO-*d*₆) δ 0.76 (s, 3H), 1.11 (d, $J = 6.3$ Hz, 3H), 1.16 (d, $J = 6.8$ Hz, 4H), 1.24 (d, $J = 12.8$ Hz, 1H), 1.39 – 1.51 (m, 2H), 1.58 (s, 3H), 2.03 (d, $J = 12.1$ Hz, 1H), 2.33 – 2.44 (m, 1H), 2.59 – 2.66 (m, 1H), 2.67 (s, 3H), 2.69 – 2.75 (m, 1H), 2.78 (d, $J = 9.7$ Hz, 2H), 3.07 (s, 3H), 3.16 (d, $J = 12.7$ Hz, 1H), 3.24 (s, 3H), 3.48 (d, $J = 9.0$ Hz, 1H), 3.60 (d, $J = 7.9$ Hz, 1H), 3.64 (s, 1H), 3.94 (s, 3H), 4.01 (d, $J = 5.6$ Hz, 2H), 4.02 – 4.11 (m, 2H), 4.51 (dd, $J = 12.0, 2.5$ Hz, 1H), 5.30 (q, $J = 6.7$ Hz, 1H), 5.55 (dd, $J = 12.9, 10.1$ Hz, 1H), 5.92 (s, 1H), 6.50 – 6.60 (m, 4H), 6.88 (s, 1H), 7.10 (d, $J = 8.4$ Hz, 2H), 7.19 (s, 1H), 7.49 (d, $J = 8.4$ Hz, 2H), 8.10 – 8.33 (m, 1H), 8.80 (t, $J = 5.6$

1
2
3 Hz, 1H), 10.21 (s, 1H). ^{13}C NMR (101 MHz, DMSO) δ 11.36, 13.07, 14.41, 15.04, 23.52, 26.05,
4 29.70, 31.92, 33.37, 34.86, 35.18, 36.34, 37.69, 37.71, 38.89, 39.10, 39.31, 39.52, 39.73, 39.94,
5 40.15, 42.68, 45.42, 51.64, 56.11, 56.60, 60.01, 66.74, 73.15, 77.63, 79.99, 88.18, 113.95,
6 117.12, 119.13, 121.60, 125.13, 128.46, 128.94, 132.58, 133.35, 134.15, 137.44, 138.35, 141.26,
7 151.22, 155.26, 166.39, 166.98, 168.11, 170.60. HRMS ($\text{M} + \text{Na}$) $^+$ 979.3655, found 979.3618.
8
9
10

11
12 **General procedure for the preparation of compounds (17a – 17f).** One of the dipeptide
13 compounds (16a – 16f) (0.077 mmol) was dissolved in DMF (1 mL) to which was added SPDB
14 (65 mg, 0.2 mmol). After 1 h the reaction solution was purified by the preparative HPLC
15 method 1. Fractions containing desired product were combined in a 100 mL flask, frozen in a
16 dry ice acetone bath then lyophilized.
17
18
19

20 **SPDB-*L*-Ala-*L*-Ala-PA-May (17e).** White solid (69% yield). ^1H NMR (400 MHz, DMSO- d_6)
21 δ 0.77 (s, 3H), 1.12 (d, $J = 6.3$ Hz, 3H), 1.16 (d, $J = 6.8$ Hz, 3H), 1.20 (d, $J = 7.0$ Hz, 3H), 1.30
22 (d, $J = 7.0$ Hz, 3H), 1.40 – 1.50 (m, 3H), 1.58 (s, 3H), 1.86 (p, $J = 7.2$ Hz, 2H), 2.03 (dd, $J =$
23 14.4, 2.9 Hz, 1H), 2.27 (t, $J = 7.2$ Hz, 2H), 2.38 (ddd, $J = 16.2, 8.2, 5.9$ Hz, 1H), 2.62 (dd, $J =$
24 14.8, 7.1 Hz, 2H), 2.67 (s, 3H), 2.70 – 2.77 (m, 2H), 2.79 (d, $J = 9.7$ Hz, 1H), 2.83 (t, $J = 7.3$ Hz,
25 2H), 3.07 (s, 3H), 3.13 (d, $J = 12.6$ Hz, 1H), 3.25 (s, 3H), 3.38 (d, $J = 12.3$ Hz, 2H), 3.48 (d, $J =$
26 8.9 Hz, 1H), 3.55 – 3.66 (m, 2H), 3.93 (s, 3H), 4.02 – 4.12 (m, 1H), 4.25 (p, $J = 7.0$ Hz, 1H),
27 4.38 (p, $J = 7.0$ Hz, 1H), 4.52 (dd, $J = 11.9, 2.9$ Hz, 1H), 5.27 – 5.34 (m, 1H), 5.56 (dd, $J = 13.6,$
28 9.0 Hz, 1H), 5.93 (s, 1H), 6.49 – 6.64 (m, 2H), 6.87 (s, 1H), 7.09 (d, $J = 8.4$ Hz, 2H), 7.15 (d, $J =$
29 1.7 Hz, 1H), 7.21 (ddd, $J = 7.0, 4.7, 1.2$ Hz, 1H), 7.48 – 7.53 (m, 2H), 7.73 – 7.84 (m, 2H), 8.10
30 (dd, $J = 7.1, 3.6$ Hz, 2H), 8.41 – 8.47 (m, 1H), 9.85 (s, 1H). ^{13}C NMR (101 MHz, DMSO) δ
31 172.43, 171.75, 170.93, 170.56, 168.10, 159.28, 155.25, 151.24, 149.50, 141.25, 138.33, 137.69,
32 137.45, 133.33, 132.59, 128.86, 128.46, 125.14, 121.57, 121.04, 119.21, 119.09, 117.12, 113.89,
33 88.20, 79.99, 77.63, 73.16, 66.76, 60.00, 56.53, 56.10, 51.65, 48.96, 48.92, 48.74, 45.43, 37.70,
34 37.38, 36.35, 35.17, 34.87, 33.33, 33.28, 31.92, 29.69, 25.98, 24.51, 17.89, 17.53, 15.02, 14.41,
35 13.06, 11.37. HRMS ($\text{M} + \text{Na}$) $^+$ calcd. 1218.4093, found 1218.4062.
36
37
38
39
40
41

42 **SPDB-*L*-Val-*L*-Cit-PA-May (17a).** White solid (71% yield). ^1H NMR (400 MHz, Acetonitrile-
43 d_3) δ 0.75 (s, 3H), 0.86 (d, $J = 5.0$ Hz, 3H), 0.88 (d, $J = 5.0$ Hz, 3H), 1.15 (d, $J = 6.4$ Hz, 3H),
44 1.19 (d, $J = 6.9$ Hz, 3H), 1.31 – 1.49 (m, 4H), 1.58 (s, 3H), 1.87 – 1.91 (m, 2H), 2.36 (dt, $J = 7.6,$
45 6.5 Hz, 5H), 2.50 – 2.66 (m, 4H), 2.68 (s, 3H), 2.76 – 2.91 (m, 5H), 2.99 – 3.07 (m, 3H), 3.08 (s,
46 3H), 3.28 (s, 3H), 3.41 – 3.53 (m, 2H), 3.59 (d, $J = 2.9$ Hz, 2H), 3.92 (s, 3H), 4.04 – 4.16 (m,
47 2H), 4.39 (dd, $J = 9.3, 4.7$ Hz, 1H), 4.55 (dd, $J = 12.1, 3.0$ Hz, 1H), 5.32 (q, $J = 6.8$ Hz, 1H), 5.59
48 (dd, $J = 14.1, 9.1$ Hz, 1H), 6.40 – 6.61 (m, 2H), 7.01 – 7.50 (m, 10H), 7.58 – 7.87 (m, 6H), 8.35
49 – 8.43 (m, 3H). HRMS ($\text{M} + \text{Na}$) $^+$ calcd. 1332.4886, found 1332.4828
50
51
52
53

54 **SPDB-*D*-Ala-*D*-Ala-PA-May (17b).** White solid (64% yield). ^1H NMR (400 MHz, DMSO- d_6)
55 δ 0.76 (s, 3H), 1.12 (d, $J = 6.3$ Hz, 3H), 1.16 (d, $J = 6.8$ Hz, 3H), 1.20 (d, $J = 7.1$ Hz, 3H), 1.30
56 (d, $J = 7.1$ Hz, 3H), 1.44 (dd, $J = 15.0, 8.8$ Hz, 2H), 1.57 (s, 3H), 1.79 – 1.92 (m, 2H), 2.03 (d, J
57
58
59
60

1
2
3 = 11.9 Hz, 1H), 2.26 (t, $J = 7.2$ Hz, 2H), 2.31 – 2.43 (m, 1H), 2.67 (s, 5H), 2.75 – 2.89 (m, 4H),
4 3.07 (s, 3H), 3.13 (d, $J = 12.5$ Hz, 1H), 3.24 (s, 3H), 3.48 (d, $J = 9.0$ Hz, 1H), 3.60 (d, $J = 6.9$ Hz,
5 2H), 3.93 (s, 3H), 4.06 (t, $J = 10.5$ Hz, 1H), 4.19 – 4.29 (m, 1H), 4.31 – 4.43 (m, 1H), 4.51 (dd, J
6 = 12.0, 2.6 Hz, 1H), 5.30 (q, $J = 6.6$ Hz, 1H), 5.55 (dd, $J = 13.5, 9.7$ Hz, 1H), 5.92 (s, 1H), 6.47 –
7 6.61 (m, 3H), 6.87 (s, 1H), 7.09 (d, $J = 8.5$ Hz, 2H), 7.15 (d, $J = 1.4$ Hz, 1H), 7.22 (ddd, $J = 7.2,$
8 4.8, 1.2 Hz, 1H), 7.48 (d, $J = 8.5$ Hz, 2H), 7.72 – 7.86 (m, 2H), 8.09 (d, $J = 7.0$ Hz, 2H), 8.42 –
9 8.50 (m, 1H), 9.82 (s, 1H). HRMS (M + Na)⁺ calcd 1218.4093 found 1218.4061.

10
11
12
13 **SPDB-D-Ala-L-Ala-PA-May (17c).** White solid (62% yield). ¹H NMR (400 MHz, DMSO-d₆)
14 δ 0.76 (s, 3H), 1.12 (d, $J = 6.4$ Hz, 3H), 1.16 (d, $J = 6.8$ Hz, 3H), 1.20 (d, $J = 7.0$ Hz, 3H), 1.22 –
15 1.27 (m, 1H), 1.31 (d, $J = 7.1$ Hz, 3H), 1.40 – 1.50 (m, 2H), 1.57 (s, 3H), 1.85 (p, $J = 7.3$ Hz,
16 2H), 2.03 (dd, $J = 14.4, 2.9$ Hz, 1H), 2.27 (t, $J = 7.2$ Hz, 2H), 2.32 – 2.44 (m, 1H), 2.63 (dd, $J =$
17 13.7, 6.5 Hz, 1H), 2.67 (s, 3H), 2.69 – 2.77 (m, 1H), 2.80 (td, $J = 9.5, 8.8, 4.1$ Hz, 3H), 3.07 (s,
18 3H), 3.12 (dd, $J = 12.9, 4.1$ Hz, 1H), 3.24 (s, 3H), 3.48 (d, $J = 9.1$ Hz, 1H), 3.54 – 3.66 (m, 2H),
19 3.93 (s, 3H), 4.02 – 4.11 (m, 1H), 4.22 (t, $J = 6.8$ Hz, 1H), 4.36 (td, $J = 7.4, 1.6$ Hz, 1H), 4.52
20 (dd, $J = 11.9, 2.9$ Hz, 1H), 5.30 (q, $J = 6.8$ Hz, 1H), 5.56 (dd, $J = 13.4, 9.1$ Hz, 1H), 5.93 (s, 1H),
21 6.48 – 6.54 (m, 2H), 6.57 (d, $J = 11.3$ Hz, 2H), 6.87 (s, 1H), 7.10 (dd, $J = 8.6, 2.1$ Hz, 2H), 7.12
22 – 7.17 (m, 1H), 7.20 (dd, $J = 7.2, 4.8$ Hz, 1H), 7.56 (dd, $J = 8.5, 2.6$ Hz, 2H), 7.70 – 7.83 (m,
23 2H), 8.22 (d, $J = 6.3$ Hz, 1H), 8.38 (dd, $J = 7.6, 3.9$ Hz, 1H), 8.41 – 8.45 (m, 1H), 9.69 (d, $J = 3.5$
24 Hz, 1H). ¹³C NMR (101 MHz, DMSO) δ 172.44, 172.42, 171.75, 170.95, 170.59, 170.56,
25 168.11, 159.28, 155.25, 151.24, 149.51, 141.26, 138.33, 137.71, 137.47, 133.35, 133.34, 132.59,
26 128.89, 128.87, 128.47, 125.15, 121.58, 121.06, 119.22, 119.10, 117.13, 113.90, 88.20, 79.99,
27 77.64, 73.16, 66.77, 60.01, 56.54, 56.11, 51.65, 48.96, 48.93, 48.74, 45.43, 37.70, 37.38, 36.35,
28 35.18, 34.87, 33.34, 33.29, 31.92, 29.69, 26.00, 24.51, 17.90, 17.54, 15.03, 14.41, 13.06, 11.37.
29 HRMS (M + Na)⁺ calcd. 1218.4093, found 1218.4062.

30
31
32
33 **SPDB-L-Ala-D-Ala-PA-May (17d).** White solid (66 % yield). ¹H NMR (400 MHz, DMSO-d₆)
34 δ 0.76 (s, 3H), 1.12 (d, $J = 6.2$ Hz, 3H), 1.16 (d, $J = 6.8$ Hz, 3H), 1.20 (d, $J = 7.1$ Hz, 3H), 1.24
35 (d, $J = 13.6$ Hz, 1H), 1.31 (d, $J = 7.2$ Hz, 3H), 1.39 – 1.51 (m, 3H), 1.58 (d, $J = 5.7$ Hz, 3H), 1.86
36 (p, $J = 7.2$ Hz, 3H), 2.00 – 2.08 (m, 1H), 2.27 (t, $J = 7.2$ Hz, 2H), 2.38 (ddd, $J = 15.8, 8.0, 5.8$
37 Hz, 1H), 2.63 (dd, $J = 13.8, 6.4$ Hz, 1H), 2.67 (s, 3H), 2.76 – 2.86 (m, 4H), 3.07 (s, 3H), 3.24 (s,
38 3H), 3.48 (d, $J = 8.9$ Hz, 1H), 3.54 – 3.66 (m, 2H), 3.93 (s, 3H), 4.02 – 4.11 (m, 1H), 4.22 (dt, J
39 = 13.9, 6.8 Hz, 1H), 4.32 – 4.40 (m, 1H), 4.52 (dd, $J = 11.9, 2.9$ Hz, 1H), 5.31 (q, $J = 6.8$ Hz,
40 2H), 5.56 (dd, $J = 13.7, 9.0$ Hz, 1H), 5.93 (s, 1H), 6.48 – 6.61 (m, 2H), 6.89 (d, $J = 6.9$ Hz, 1H),
41 7.10 (dd, $J = 8.6, 2.1$ Hz, 2H), 7.18 – 7.25 (m, 1H), 7.56 (m, 2H), 7.70 – 7.83 (m, 2H), 8.21 (d, J
42 = 6.2 Hz, 2H), 8.38 (d, $J = 7.6$ Hz, 1H), 8.41 – 8.46 (m, 1H), 9.68 (s, 1H). ¹³C NMR (101 MHz,
43 DMSO) δ 172.43, 171.75, 170.93, 170.56, 168.10, 159.28, 155.25, 151.24, 149.50, 141.25,
44 138.33, 137.69, 137.45, 133.33, 132.59, 128.86, 128.46, 125.14, 121.57, 121.04, 119.21, 119.09,
45 117.12, 113.89, 88.20, 79.99, 77.63, 73.16, 66.76, 60.00, 56.53, 56.10, 51.65, 48.96, 48.92,
46 48.74, 45.43, 37.70, 37.38, 36.35, 35.17, 34.87, 33.33, 33.28, 31.92, 29.69, 25.98, 24.51, 17.89,
47 17.53, 15.02, 14.41, 13.06, 11.37. HRMS (M + Na)⁺ calcd. 1218.4093, found 1218.4058.
48
49
50
51
52
53
54
55
56
57
58
59
60

1
2
3
4
5 **SPDB-Gly-Gly-PA-May (17f)**. White solid (61 % yield). ^1H NMR (400 MHz, DMSO- d_6) δ
6 0.78 (s, 3H), 1.13 (d, $J = 6.3$ Hz, 3H), 1.17 (d, $J = 6.7$ Hz, 3H), 1.24 (d, $J = 13.0$ Hz, 1H), 1.46
7 (dd, $J = 14.9, 8.3$ Hz, 2H), 1.58 (s, 2H), 1.77 (dd, $J = 14.3, 7.1$ Hz, 2H), 2.03 (d, $J = 14.0$ Hz,
8 1H), 2.28 (t, $J = 7.2$ Hz, 3H), 2.33 – 2.43 (m, 1H), 2.69 (s, 3H), 2.79 (d, $J = 9.5$ Hz, 1H), 3.06 (s,
9 3H), 3.12 (d, $J = 12.5$ Hz, 1H), 3.27 (s, 3H), 3.49 (d, $J = 9.0$ Hz, 1H), 3.61 (d, $J = 7.3$ Hz, 1H),
10 3.71 (d, $J = 5.5$ Hz, 2H), 3.87 (d, $J = 5.6$ Hz, 2H), 3.94 (s, 3H), 4.08 (t, $J = 11.0$ Hz, 1H), 4.50 (d,
11 $J = 11.7$ Hz, 1H), 5.23 – 5.29 (m, 1H), 5.50 – 5.58 (m, 1H), 5.94 (s, 1H), 6.47 – 6.56 (m, 3H),
12 6.89 (s, 1H), 7.11 (d, $J = 8.4$ Hz, 2H), 7.15 (s, 1H), 7.22 (dd, $J = 7.2, 4.6$ Hz, 1H), 7.49 (d, $J =$
13 8.4 Hz, 2H), 7.69 – 7.830 (m, 2H), 8.19 – 8.29 (m, 2H), 8.35 (dd, $J = 7.6, 3.9$ Hz, 1H), 8.77 (s,
14 1H). HRMS ($M + \text{Na}$) $^+$ calcd. 1190.3775, found 1190.3778.
15
16
17
18

19 **General Procedure for the preparation of thiol-bearing maytansinoids (18a – 18f)**. One of
20 the compounds (**17a – 17f**) (0.043 mmol) was taken up in a solution of DMSO (300 μL) and 50
21 mM potassium phosphate buffer pH 7.4 (100 μL) containing dithiothreitol (35 mg, 0.21 mmol).
22 After 1 h the slightly yellow reaction was purified by preparative C18 HPLC 1. Fractions
23 containing desired product were combined as quickly as possible in a 100 mL flask, frozen in a
24 dry ice acetone bath then lyophilized. It should be noted that a small amount of symmetric
25 disulfide dimer can form during NMR analysis or conjugation, however the resulting disulfide
26 can not be conjugated to antibodies by reaction with the maleimide moiety of sulfo-GMB.
27 Samples should be stored under an inert atmosphere.
28
29
30
31

32 **HS-L-Val-L-Cit-PA-May (18a)**. Fluffy white solid prone to static (70 % yield). ^1H NMR (400
33 MHz, DMSO- d_6) δ 0.76 (s, 3H), 0.85 (d, $J = 6.8$ Hz, 3H), 0.87 (d, $J = 6.7$ Hz, 3H), 1.13 (d, $J =$
34 6.2 Hz, 3H), 1.17 (d, $J = 6.7$ Hz, 3H), 1.21 – 1.30 (m, 1H), 1.35 – 1.48 (m, 4H), 1.58 (s, 3H),
35 1.61-1.64 (m, 1H), 1.69 – 1.83 (m, 3H), 1.95 – 2.10 (m, 2H), 2.24 – 2.35 (m, 3H), 2.39 – 2.45
36 (m, 2H), 2.52 – 2.54 (m, 1H), 2.56 – 2.65 (m, 1H), 2.68 (s, 3H), 2.70 – 2.84 (m, 2H), 2.93 – 3.07
37 (m, 2H), 3.09 (s, 3H), 3.10 – 3.15 (m, 1H), 3.26 (s, 3H), 3.33 - 3.65 (m, 6H), 3.93 (s, 3H), 4.04 –
38 4.13 (m, 1H), 4.16 – 4.23 (m, 1H), 4.41 (dd, $J = 13.3, 7.8$ Hz, 1H), 4.53 (dd, $J = 11.7, 2.1$ Hz,
39 1H), 5.32 (dd, $J = 12.6, 5.7$ Hz, 1H), 5.37 (s, 2H), 5.57 (dd, $J = 14.8, 8.8$ Hz, 1H), 5.91 – 6.02
40 (m, 2H), 6.45 – 6.61 (m, 3H), 6.78 (s, 1H), 7.04 – 7.11 (m, 2H), 7.15 (s, 1H), 7.48 (d, $J = 8.2$ Hz,
41 2H), 7.85 (d, $J = 8.7$ Hz, 1H), 8.04 (d, $J = 7.6$ Hz, 1H), 9.88 (s, 1H). HRMS ($M + \text{Na}$) $^+$ calcd.
42 1223.4900, found 1223.4790.
43
44
45
46
47

48 **HS-D-Ala-D-Ala-PA-May (18b)**. Fluffy white solid prone to static (65 % yield). ^1H NMR (400
49 MHz, DMSO- d_6) δ 0.76 (s, 3H), 1.12 (d, $J = 6.3$ Hz, 3H), 1.16 (d, $J = 6.8$ Hz, 3H), 1.21 (d, $J =$
50 7.1 Hz, 3H), 1.31 (d, $J = 7.0$ Hz, 3H), 1.39 – 1.51 (m, 2H), 1.58 (s, 3H), 1.76 (p, $J = 7.2$ Hz, 2H),
51 2.03 (dd, $J = 14.4, 2.8$ Hz, 1H), 2.19 – 2.31 (m, 3H), 2.30 – 2.44 (m, 1H), 2.44 – 2.47 (m, 2H),
52 2.57 – 2.67 (m, 1H), 2.67 (s, 3H), 2.78 (d, $J = 9.7$ Hz, 1H), 3.07 (s, 3H), 3.13 (d, $J = 12.6$ Hz,
53 1H), 3.24 (d, $J = 2.5$ Hz, 3H), 3.37 (d, $J = 12.5$ Hz, 1H), 3.48 (d, $J = 9.1$ Hz, 1H), 3.53 – 3.67 (m,
54 2H), 3.94 (s, 3H), 4.06 (td, $J = 11.3, 10.3, 2.2$ Hz, 1H), 4.22 – 4.31 (m, 1H), 4.33 – 4.40 (m, 1H),
55 4.52 (dd, $J = 12.0, 2.9$ Hz, 1H), 5.30 (q, $J = 6.6$ Hz, 1H), 5.50 – 5.61 (m, 1H), 5.92 (d, $J = 1.4$
56
57
58
59
60

1
2
3 Hz, 1H), 6.48 – 6.58 (m, 3H), 6.87 (s, 1H), 7.05 – 7.13 (m, 2H), 7.16 (d, $J = 1.9$ Hz, 1H), 7.44 –
4 7.52 (m, 2H), 8.02 – 8.12 (m, 2H), 9.83 (s, 1H). HRMS (M + Na)⁺ calcd. 1109.4107, found
5 1109.4073.
6
7

8 **HS-D-Ala-L-Ala-PA-May (18c).** Fluffy white solid prone to static (81 % yield). ¹H NMR (400
9 MHz, DMSO-d₆) δ 0.77 (s, 3H), 1.12 (d, $J = 6.4$ Hz, 3H), 1.16 (d, $J = 6.8$ Hz, 3H), 1.21 (d, $J =$
10 7.0 Hz, 3H), 1.31 (d, $J = 7.1$ Hz, 3H), 1.44 (td, $J = 10.7, 9.9, 5.6$ Hz, 2H), 1.58 (s, 3H), 1.68 –
11 1.80 (m, 2H), 2.03 (dd, $J = 14.5, 2.9$ Hz, 1H), 2.15 – 2.28 (m, 3H), 2.31 – 2.49 (m, 4H), 2.58 –
12 2.62 (m, 1H), 2.67 (s, 3H), 2.73 – 2.80 (m, 2H), 3.07 (s, 3H), 3.09 – 3.16 (m, 1H), 3.25 (s, 3H),
13 3.36-3.43 (m, 3H), 3.48 (d, $J = 9.0$ Hz, 1H), 3.53-3.67 (m, 2H), 3.93 (s, 3H), 4.01 – 4.12 (m,
14 1H), 4.24 (q, $J = 6.7$ Hz, 1H), 4.36 (qd, $J = 7.8, 5.9$ Hz, 1H), 4.52 (dd, $J = 12.0, 2.9$ Hz, 1H), 5.30
15 (q, $J = 6.7$ Hz, 1H), 5.56 (dd, $J = 13.4, 9.0$ Hz, 1H), 5.92 (s, 1H), 6.47 – 6.61 (m, 3H), 6.87 (s,
16 1H), 7.10 (dd, $J = 8.5, 2.3$ Hz, 2H), 7.14 – 7.18 (m, 1H), 7.56 (dd, $J = 8.6, 2.4$ Hz, 2H), 8.17 (d, $J =$
17 = 6.4 Hz, 1H), 8.36 (dd, $J = 7.5, 5.1$ Hz, 1H), 9.68 (d, $J = 4.7$ Hz, 1H). ¹³C NMR (101 MHz,
18 DMSO) δ 172.42, 171.95, 170.91, 170.53, 168.08, 155.23, 151.20, 141.23, 138.31, 137.42,
19 133.35, 132.56, 128.86, 128.44, 125.11, 121.56, 119.20, 117.10, 113.88, 99.50, 88.19, 79.96,
20 77.61, 73.14, 66.74, 59.98, 56.52, 56.09, 51.62, 48.91, 48.68, 37.68, 35.17, 34.83, 33.44, 31.91,
21 29.67, 29.48, 25.98, 23.36, 17.90, 17.56, 15.01, 14.39, 13.04, 11.35. HRMS (M + Na)⁺ calcd.
22 1109.4107, found 1109.4076.
23
24
25
26
27
28

29 **HS-L-Ala-D-Ala-PA-May (18d).** Fluffy white solid prone to static (80 % yield). ¹H NMR (400
30 MHz, DMSO-d₆) δ 0.76 (s, 3H), 1.12 (d, $J = 6.3$ Hz, 3H), 1.16 (d, $J = 6.7$ Hz, 3H), 1.21 (d, $J =$
31 7.1 Hz, 3H), 1.31 (d, $J = 7.0$ Hz, 3H), 1.39 – 1.50 (m, 2H), 1.58 (s, 3H), 1.75 (p, $J = 7.2$ Hz, 2H),
32 2.03 (dd, $J = 14.4, 2.8$ Hz, 1H), 2.14 – 2.21 (m, 1H), 2.24 (t, $J = 7.3$ Hz, 2H), 2.32 – 2.46 (m,
33 3H), 2.52 – 2.55 (m, 1H), 2.58 – 2.64 (m, 1H), 2.70 – 2.74 (m, 1H), 2.74 – 2.81 (m, 1H), 3.08 (s,
34 3H), 3.12 (d, $J = 12.7$ Hz, 1H), 3.25 (s, 3H), 3.32 – 3.42 (m, 1H), 3.48 (d, $J = 9.0$ Hz, 1H), 3.54 –
35 3.66 (m, 2H), 3.93 (s, 3H), 4.06 (t, $J = 11.4$ Hz, 1H), 4.23 (p, $J = 6.9$ Hz, 1H), 4.36 (p, $J = 7.2$
36 Hz, 1H), 4.52 (dd, $J = 11.9, 2.9$ Hz, 1H), 5.30 (q, $J = 6.8$ Hz, 1H), 5.56 (dd, $J = 13.5, 9.2$ Hz,
37 1H), 5.92 (s, 1H), 6.48 – 6.54 (m, 3H), 6.87 (s, 1H), 7.10 (d, $J = 8.3$ Hz, 2H), 7.12 – 7.17 (m,
38 1H), 7.56 (dd, $J = 8.6, 2.6$ Hz, 2H), 8.18 (d, $J = 6.4$ Hz, 1H), 8.36 (t, $J = 6.5$ Hz, 1H), 9.68 (s,
39 1H). ¹³C NMR (101 MHz, DMSO) δ 172.48, 172.01, 171.99, 170.93, 170.55, 168.09, 155.25,
40 151.23, 141.25, 138.34, 137.45, 133.32, 132.59, 128.87, 128.84, 128.44, 125.12, 121.57, 119.23,
41 117.13, 113.88, 88.22, 79.98, 77.62, 73.16, 66.76, 59.98, 56.52, 56.10, 51.64, 48.95, 48.74,
42 45.43, 37.71, 36.35, 35.17, 34.86, 33.45, 33.34, 31.91, 29.68, 29.50, 25.96, 23.39, 17.89, 17.53,
43 15.02, 14.40, 13.06, 11.38. HRMS (M + Na)⁺ calcd. 1109.4107, found 1109.4078.
44
45
46
47
48
49

50 **HS-L-Ala-L-Ala-PA-May (18e).** Fluffy white solid prone to static (75 % yield). ¹H NMR (400
51 MHz, DMSO-d₆) δ 0.77 (s, 3H), 1.12 (d, $J = 6.3$ Hz, 3H), 1.16 (d, $J = 6.8$ Hz, 3H), 1.21 (d, $J =$
52 7.2 Hz, 3H), 1.25 (m, 1H), 1.31 (d, $J = 7.0$ Hz, 3H), 1.44 (td, $J = 10.5, 9.9, 4.8$ Hz, 2H), 1.58 (s,
53 3H), 1.76 (p, $J = 7.2$ Hz, 2H), 2.03 (dd, $J = 14.4, 2.7$ Hz, 1H), 2.19 – 2.28 (m, 3H), 2.31 – 2.38
54 (m, 1H), 2.43 – 2.48 (m, 2H), 2.51 – 2.57 (m, 1H), 2.62 (q, $J = 7.8, 6.5$ Hz, 1H), 2.67 (s, 3H),
55 2.71 – 2.75 (m, 1H), 2.79 (d, $J = 9.6$ Hz, 1H), 3.07 (s, 3H), 3.13 (d, $J = 12.5$ Hz, 1H), 3.25 (s,
56
57
58
59
60

3H), 3.30 – 3.42 (m, 1H), 3.48 (d, $J = 9.0$ Hz, 1H), 3.54 – 3.66 (m, 2H), 3.94 (s, 3H), 4.02 – 4.12 (m, 1H), 4.27 (p, $J = 7.1$ Hz, 1H), 4.38 (p, $J = 7.1$ Hz, 1H), 4.52 (dd, $J = 11.9, 2.8$ Hz, 1H), 5.31 (q, $J = 6.8$ Hz, 1H), 5.56 (dd, $J = 13.5, 9.1$ Hz, 1H), 5.92 (s, 1H), 6.48 – 6.60 (m, 3H), 6.87 (s, 1H), 7.09 (d, $J = 8.3$ Hz, 2H), 7.15 (s, 1H), 7.50 (d, $J = 8.3$ Hz, 2H), 8.08 (dd, $J = 10.2, 7.1$ Hz, 2H), 9.85 (s, 1H). ^{13}C NMR (101 MHz, DMSO) δ 172.23, 171.71, 171.00, 170.57, 170.54, 168.09, 155.25, 151.23, 141.26, 141.23, 138.30, 137.59, 133.22, 132.58, 128.92, 128.45, 125.14, 121.58, 119.03, 117.14, 113.89, 88.20, 79.98, 77.63, 73.15, 66.76, 59.98, 56.53, 56.10, 51.64, 48.94, 48.27, 45.42, 37.70, 36.34, 35.17, 34.88, 33.68, 33.33, 31.91, 29.68, 29.52, 25.97, 23.44, 18.04, 17.90, 15.02, 14.40, 13.05, 11.37. HRMS (M + Na)⁺ calcd. 1109.4107, found 1109.4082.

HS-Gly-Gly-PA-May (18f). Fluffy white solid prone to static (69 % yield). ^1H NMR (400 MHz, DMSO- d_6) δ 0.77 (s, 3H), 1.12 (d, $J = 6.3$ Hz, 3H), 1.16 (d, $J = 6.7$ Hz, 3H), 1.24 (d, $J = 13.1$ Hz, 1H), 1.45 (dd, $J = 14.9, 8.2$ Hz, 2H), 1.58 (s, 3H), 1.79 (dd, $J = 14.3, 7.2$ Hz, 2H), 2.03 (d, $J = 14.0$ Hz, 1H), 2.27 (t, $J = 7.3$ Hz, 3H), 2.33 – 2.45 (m, 1H), 2.53 – 2.57 (m, 2H), 2.67 (s, 3H), 2.70 – 2.82 (m, 3H), 3.07 (s, 3H), 3.14 (d, $J = 12.6$ Hz, 1H), 3.25 (s, 3H), 3.48 (d, $J = 9.0$ Hz, 1H), 3.60 (d, $J = 7.2$ Hz, 1H), 3.73 (d, $J = 5.6$ Hz, 2H), 3.88 (d, $J = 5.7$ Hz, 2H), 3.93 (s, 3H), 4.06 (t, $J = 11.2$ Hz, 1H), 4.52 (d, $J = 11.9$ Hz, 1H), 5.26 – 5.34 (m, 1H), 5.52 – 5.60 (m, 1H), 5.92 (s, 1H), 6.49 – 6.60 (m, 3H), 6.87 (s, 1H), 7.10 (d, $J = 8.5$ Hz, 2H), 7.16 (s, 1H), 7.49 (d, $J = 8.4$ Hz, 2H), 8.19 – 8.29 (m, 2H), 9.76 (s, 1H). HRMS (M + Na)⁺ calcd. 1081.3794, found 1081.3740.

General procedure for the preparation of AaMCs.

Preparation of Maytansinoid solution. Sulfo-GMBS and one of the thiol-bearing maytansinoids (**18a** – **18f**) were dissolved in a solution of 3:7 (50 mM sodium succinate, pH 5.0: DMA) to give a concentration of 1.5 mM and 1.9 mM of each respectively. The solution was gently stirred at room temperature for 30 min then excess thiol was quenched by bringing the solution to 0.5 mM in *N*-ethyl maleimide (NEM) with gentle stirring for 10 min.

Preparation of AaMCs. To a solution of the antibody (2.5 mg/mL) in 60 mM EPPS containing 15 % by volume *N,N*-dimethyl acetamide (DMA), pH 8.0 was added 6.5 mole eq. of maytansinoid solution. After 16 h the reaction mixture was purified using a NAP-G25 column that was pre-equilibrated and run with 10 mM sodium succinate, pH 5.5, 250 mM glycine, 0.5% sucrose, and 0.01% Tween-20 buffer. The purified conjugate was analyzed to determine the maytansinoid per antibody ratio (MAR), percent aggregated conjugate, free maytansinoid levels and endotoxin units (EU) as previously described.²¹ Protein aggregate levels in all conjugates were below 3%, free maytansinoid levels were below 1% and endotoxin levels were below 0.2 EU/mg. The maytansinoid to antibody ratio (MAR) values for each AaMC were as follows **8a** MAR = 3.8, **8b** MAR = 3.9, **8c** MAR = 4.1, **8d** MAR = 4.1, **8e** MAR = 3.8, **8f** MAR = 3.8, **8g** MAR = 4.1, **8h** MAR = 3.7, **8i** MAR = 3.9.

In vitro experiments.

1
2
3 ***In vitro cytotoxicity assays (WST-8).*** Assays were performed in flat bottom 96-well plates in
4 triplicate for each data point. In brief, test articles were first diluted in complete cell culture
5 media using 5-fold dilution series and 100 μL were added into each well. The final
6 concentrations typically ranged from 3×10^{-8} M to 8×10^{-14} M. The target cells were then added
7 to the test articles at 1,500 to 3,000 cells per well in 100 μL of complete culture media. The
8 mixtures were incubated at 37 °C in a humidified 5% CO_2 incubator for 5 days. Viability of the
9 remaining cells was determined by the WST-8 (Tetrazolium salt-8; 2-(2-methoxy-4-
10 nitrophenyl)-3-(4-nitrophenyl)-5-(2,4-disulfophenyl)-2H-tetrazolium) based colorimetric assay
11 using the Cell Counting Kit-8 (Dojindo Molecular Technologies, Inc., Rockville, MD). The
12 WST-8 is reduced by dehydrogenases in live cells to give a yellow-colored formazan product
13 that is soluble in tissue culture media. The amount of formazan dye is directly proportional to the
14 number of live cells. The WST-8 was added to a final volume of 10% and plates were incubated
15 at 37°C in a humidified 5% CO_2 incubator for an additional 4 h. The WST-8 signals were then
16 measured using a microplate plate reader at optical density of 450 nm. The surviving fraction
17 was calculated by dividing the value of each treated sample by the average value of untreated
18 controls, and plotted against the test article concentrations in a semi-log plot for each treatment.
19 IC_{50} values were determined using nonlinear regression (curve fit) with GraphPad Prism v5
20 program (GraphPad Software, La Jolla, CA).
21
22
23
24
25
26
27

28
29 ***In vitro cell cycle arrest assays.*** Assays for bafilomycin A1 inhibition of cell cycle arrest in the
30 presence of conjugate were conducted at a varying concentrations of conjugate with or without
31 bafilomycin A at a final concentration of 7 nM by a previously described procedure.¹
32
33

34 ***In vitro bystander killing assays.*** Bystander killing assays in which the number of antigen-
35 negative cells are held constant in the presence of varying numbers of antigen-positive cells were
36 conducted as described previously using the ratio of antigen-positive to antigen-negative cells
37 designated in the relevant figures.¹¹ A variation on this assay in which antigen-negative and
38 antigen-positive cells were held constant was perform as follows: 3000 EGFR+ Ca9-22 cells
39 were mixed with 2000 EGFR- MCF7 cells and the cell mixture was incubated with 0.66 nM of
40 the indicated ADCs for 4 days. The viable cells were quantified using the WST-8 assay. In the
41 same assay, the cytotoxic potency of the ADCs against Ca9-22 or MCF7 cells was also assessed;
42 all ADCs killed the EGFR+ Ca9-22 cells at a similar level but had no impact on the EGFR-
43 MCF7 cells unless antigen-positive cells were added.
44
45
46
47
48
49
50
51
52
53
54
55
56
57
58
59
60

1
2
3 **Quantitation of metabolite formation from anti-EGFR conjugate incubations with HSC-2**
4 **cells.** HSC-2 cells (1.1 million) growing in a multi-well plate were treated for about 2 h with
5 saturating 2 $\mu\text{g/mL}$ of anti-EGFR-*D-Ala-L-Ala-PA-May* (**8c**) or anti-EGFR- SPDB-DM4 (**1a**).
6 Controls included treatments with conjugates in the presence of excess unconjugated anti-EGFR
7 antibody. The cells were then washed and incubated with fresh media for another 24 h before
8 ELISA measurement of catabolites in cells and in media using a previously described
9 procedure.²⁴ The catabolite determinations, estimated from binding-competition ELISA showed
10 coefficients of variation (CV) ranging from 7-11%.
11
12
13
14

15 ***In vivo* experiments.**

16
17
18 ***In vivo* efficacy studies.** The *in vivo* efficacy of AaMC conjugates with the anti-EGFR-7R or
19 huC242 antibodies were evaluated in a homogeneously expressing non-small cell lung cancer
20 (NSCLC) tumor xenograft model, H1975, or with a heterogeneously expressing human colon
21 tumor xenograft model, HT-29, respectively. Female SCID mice were inoculated
22 subcutaneously in the right flank with the desired cell type in serum-free medium/matrigel. The
23 tumors were grown to an average size of $\sim 120 \text{ mm}^3$. The animals were then randomly divided
24 into groups (6 animals per group). Control mice were treated with phosphate-buffered saline.
25 For the homogeneously expressing H1975 xenograft study, mice were dosed at 3 mg/kg of anti-
26 EGFR-*L-Val-L-Cit-PA-May* (**8a**), anti-EGFR-*D-Ala-L-Ala-PA-May* (**8c**), anti-EGFR-*L-Ala-D-*
27 *Ala-PA-May* (**8d**), anti-EGFR-*L-Ala-L-Ala-PA-May* (**8e**) and anti-EGFR-SPDB-DM4 (**1a**). For
28 the HT-29 xenograft study, mice were treated with huC242-sulfo-SPDB-DM4 (**1b**) or huC242-
29 *D-Ala-L-Ala-PA-May* (**8c**) at 2.5 mg/kg, 5.0 mg/kg or 7.5 mg/kg. An isotype control group,
30 chKTI-*D-Ala-L-Ala-PA-May* (**8h**) was dosed at 7.5 mg/kg. All dosing in both xenograft models
31 was based on the weight of the antibody component of the conjugate. All treatments were
32 administered by tail vein intravenous injection. Tumor sizes were measured twice weekly in
33 three dimensions using a caliper with tumor volumes expressed in mm^3 and calculated using the
34 formula $V = \frac{1}{2}(\text{length} \times \text{width} \times \text{height})$. Body weight was also measured twice per week.
35
36
37
38
39
40
41
42

43 ***In vivo* tolerability of ADCs.** The acute toxicity of AaMCs and AMCs were evaluated in CD-1
44 mice based on monitoring body weight loss and clinical observations over 14 days following
45 fractionated intravenous injections via tail vein. The MTD was established when one or more
46 mice in a given group lost 20% of their pretreatment weight, or any clinical observations of
47 distress.
48
49

50 **Pharmacokinetics of AaMCs.** CD-1 mice were dosed with 10 mg/kg (intravenous, single bolus,
51 protein dose) of the indicated AaMC. Plasma samples were collected at various time intervals
52 and conjugate concentrations were measured using an ELISA assay for the antibody (irrespective
53 of maytansinoid loading), as well as for the intact conjugate (sandwich ELISA, capture the
54 maytansinoid component, detect via the antibody component). Pharmacokinetic parameters were
55 calculated using Pharsight WinNonLin software.
56
57
58
59
60

ABREVIATIONS

ADC	Antibody drug conjugate
AaMC	Antibody anilino-maytansinoid conjugate
Ala	Alanine residue
AMC	Antibody maytansinoid conjugate
Baf A1	Bafilomycin A1
huC242	humanized anti-CanAg antibody
Cit	Citruline residue
DIPEA	Diisopropyl ethylamine
DMF	Dimethylformamide
DM4	<i>N</i> ^{2'} -deacetyl- <i>N</i> ^{-2'} (4-methyl-4-mercapto-1-oxopentyl)-maytansine
DTT	1,4-dithio-DL-threitol
EDC	1-Ethyl-3-(3-dimethylaminopropyl)carbodiimide HCl salt
EEDQ	2-Ethoxy-1-ethoxycarbonyl-1,2-dihydroquinoline
EGFR	Epidermal growth factor receptor
ELISA	Enzyme-linked immunosorbent assay
Fmoc	Fluorenylmethoxycarbonyl
Gly	Glycine residue
MAR	Maytansinoid to antibody ratio
NHS	<i>N</i> -hydroxysuccinimide
PA	Para-anilino
PBD	Pyrrlobenzodiazepine
SPDB	Succinimidyl 4-(2-pyridyldithio) butyrate
Sulfo-GMBS	<i>N</i> - γ -maleimidobutyryl-oxysulfosuccinimide ester
Sulfo-SPDB	Succinimidyl 2-sulfo-4-(2-pyridyldithio)-butyrate
TI	Therapeutic index
Val	Valine residue

1
2
3
4
5
6 ASSOCIATED CONTENT
7

8 **Supporting Information**
9

10 The Supporting Information is available free of charge. Supplemental figures and pictures of ^1H
11 and ^{13}C NMRs for the final compounds used to prepare conjugates and for PA-May.
12

13
14 AUTHOR INFORMATION

15 Corresponding Author
16

17
18 *Correspondence to Wayne Widdison, ImmunoGen Inc 830 Winter street, Waltham, MA 02451.
19 Tel: (781) 0895-0713. Fax 781-895-0611. E-mail: wayne.widdison@immunogen.com
20
21
22
23
24
25
26
27
28
29
30
31
32
33
34
35
36
37
38
39
40
41
42
43
44
45
46
47
48
49
50
51
52
53
54
55
56
57
58
59
60

ACKNOWLEDGMENTS

We thank John M. Lambert and Carol Hausner for their helpful suggestions and careful reading of this manuscript.

REFERENCES

- (1) Erickson, H. K., Park, P. U., Widdison, W. C., Kovtun, Y. V., Garrett, L. M., Hoffman, K., Lutz, R. J., Goldmacher, V. S., and Blattler, W. A. (2006) Antibody-maytansinoid conjugates are activated in targeted cancer cells by lysosomal degradation and linker-dependent intracellular processing. *Cancer Res* 66, 4426-33.
- (2) Sutherland, M. S., Sanderson, R. J., Gordon, K. A., Andreyka, J., Cerveny, C. G., Yu, C., Lewis, T. S., Meyer, D. L., Zabinski, R. F., Doronina, S. O., et al. (2006) Lysosomal trafficking and cysteine protease metabolism confer target-specific cytotoxicity by peptide-linked anti-CD30-auristatin conjugates. *The Journal of biological chemistry* 281, 10540-7.
- (3) Sun, X., Widdison, W., Mayo, M., Wilhelm, S., Leece, B., Chari, R., Singh, R., and Erickson, H. (2011) Design of antibody-maytansinoid conjugates allows for efficient detoxification via liver metabolism. *Bioconjug Chem* 22, 728-35.
- (4) Sedlacek, H. H. (1992) *Antibodies as carriers of cytotoxicity*, Karger, Basel ; New York.
- (5) Heine, M., Freund, B., Nielsen, P., Jung, C., Reimer, R., Hohenberg, H., Zangemeister-Wittke, U., Wester, H. J., Luers, G. H., and Schumacher, U. (2012) High interstitial fluid pressure is associated with low tumour penetration of diagnostic monoclonal antibodies applied for molecular imaging purposes. *PLoS One* 7, e36258.
- (6) Vasalou, C., Helmlinger, G., and Gomes, B. (2015) A mechanistic tumor penetration model to guide antibody drug conjugate design. *PLoS One* 10, e0118977.
- (7) Fujimori, K., Covell, D. G., Fletcher, J. E., and Weinstein, J. N. (1989) Modeling analysis of the global and microscopic distribution of immunoglobulin G, F(ab')₂, and Fab in tumors. *Cancer Res* 49, 5656-63.
- (8) Juweid, M., Neumann, R., Paik, C., Perez-Bacete, M. J., Sato, J., van Osdol, W., and Weinstein, J. N. (1992) Micropharmacology of monoclonal antibodies in solid tumors: direct experimental evidence for a binding site barrier. *Cancer Res* 52, 5144-53.
- (9) Mitsiades, C. S., Mitsiades, N. S., Munshi, N. C., Richardson, P. G., and Anderson, K. C. (2006) The role of the bone microenvironment in the pathophysiology and therapeutic management of multiple myeloma: interplay of growth factors, their receptors and stromal interactions. *Eur J Cancer* 42, 1564-73.
- (10) Bremnes, R. M., Donnem, T., Al-Saad, S., Al-Shibli, K., Andersen, S., Sirera, R., Camps, C., Marinez, I., and Busund, L. T. (2011) The role of tumor stroma in cancer progression and prognosis: emphasis on carcinoma-associated fibroblasts and non-small cell lung cancer. *Journal of thoracic oncology : official publication of the International Association for the Study of Lung Cancer* 6, 209-17.
- (11) Kovtun, Y. V., Audette, C. A., Ye, Y., Xie, H., Ruberti, M. F., Phinney, S. J., Leece, B. A., Chittenden, T., Blaettler, W. A., and Goldmacher, V. S. (2006) Antibody-Drug

- 1
2
3
4
5
6
7
8
9
10
11
12
13
14
15
16
17
18
19
20
21
22
23
24
25
26
27
28
29
30
31
32
33
34
35
36
37
38
39
40
41
42
43
44
45
46
47
48
49
50
51
52
53
54
55
56
57
58
59
60
- Conjugates Designed to Eradicate Tumors with Homogeneous and Heterogeneous Expression of the Target Antigen. *Cancer Research* 66, 3214-3221.
- (12) Kellogg, B. A., Garrett, L., Kovtun, Y., Lai, K. C., Leece, B., Miller, M., Payne, G., Steeves, R., Whiteman, K. R., Widdison, W., et al. (2011) Disulfide-linked antibody-maytansinoid conjugates: optimization of in vivo activity by varying the steric hindrance at carbon atoms adjacent to the disulfide linkage. *Bioconjug Chem* 22, 717-27.
- (13) Ab, O., Whiteman, K. R., Bartle, L. M., Sun, X., Singh, R., Tavares, D., LaBelle, A., Payne, G., Lutz, R. J., Pinkas, J., et al. (2015) IMGN853, a Folate Receptor-alpha (FRalpha)-Targeting Antibody-Drug Conjugate, Exhibits Potent Targeted Antitumor Activity against FRalpha-Expressing Tumors. *Mol Cancer Ther* 14, 1605-13.
- (14) Okeley, N. M., Miyamoto, J. B., Zhang, X., Sanderson, R. J., Benjamin, D. R., Sievers, E. L., Senter, P. D., and Alley, S. C. (2010) Intracellular activation of SGN-35, a potent anti-CD30 antibody-drug conjugate. *Clin Cancer Res* 16, 888-97.
- (15) Borghaei, H., D., O. M., Seward, S. M., Bauer, T. M., Perez, R. P., and Oza, A. M. (2015) Phase 1 study of IMGN853, a folate receptor alpha (FR α)-targeting antibody-drug conjugate (ADC) in patients (Pts) with epithelial ovarian cancer (EOC) and other FRA-positive solid tumors. *J Clin Oncol* 33, Abstract 5558
- (16) Krop, I. E., Beeram, M., Modi, S., Jones, S. F., Holden, S. N., Yu, W., Girish, S., Tibbitts, J., Yi, J. H., Sliwkowski, M. X., et al. (2010) Phase I study of trastuzumab-DM1, an HER2 antibody-drug conjugate, given every 3 weeks to patients with HER2-positive metastatic breast cancer. *J Clin Oncol* 28, 2698-704.
- (17) Verma, S., Miles, D., Gianni, L., Krop, I. E., Welslau, M., Baselga, J., Pegram, M., Oh, D. Y., Dieras, V., Guardino, E., et al. (2012) Trastuzumab emtansine for HER2-positive advanced breast cancer. *N Engl J Med* 367, 1783-91.
- (18) Dubowchik, G. M., Firestone, R. A., Padilla, L., Willner, D., Hofstead, S. J., Mosure, K., Knipe, J. O., Lasch, S. J., and Trail, P. A. (2002) Cathepsin B-labile dipeptide linkers for lysosomal release of doxorubicin from internalizing immunoconjugates: model studies of enzymatic drug release and antigen-specific in vitro anticancer activity. *Bioconjug Chem* 13, 855-69.
- (19) Jeffrey, S. C., Burke, P. J., Lyon, R. P., Meyer, D. W., Sussman, D., Anderson, M., Hunter, J. H., Leiske, C. I., Miyamoto, J. B., Nicholas, N. D., et al. (2013) A Potent Anti-CD70 Antibody-Drug Conjugate Combining a Dimeric Pyrrolobenzodiazepine Drug with Site-Specific Conjugation Technology. *Bioconjug Chem*.
- (20) Bryson, A. (1960) The Effects of m-Substituents on the pKa Values of Anilines, and on the Stretching Frequencies of the N-H Bonds. *J. Am. Chem. Soc.* 82, 4858-4862.
- (21) Widdison Wayne, C., Wilhelm Sharon, D., Cavanagh Emily, E., Whiteman Kathleen, R., Leece Barbara, A., Kovtun, Y., Goldmacher Victor, S., Xie, H., Steeves Rita, M., Lutz Robert, J., et al. (2006) Semisynthetic maytansine analogues for the targeted treatment of cancer. *J Med Chem* 49, 4392-408.
- (22) Drose, S., and Altendorf, K. (1997) Bafilomycins and concanamycins as inhibitors of V-ATPases and P-ATPases. *The Journal of experimental biology* 200, 1-8.
- (23) van Weert, A. W., Dunn, K. W., Geuze, H. J., Maxfield, F. R., and Stoorvogel, W. (1995) Transport from late endosomes to lysosomes, but not sorting of integral membrane proteins in endosomes, depends on the vacuolar proton pump. *J Cell Biol* 130, 821-34.

- 1
2
3 (24) Salomon, P. L., and Singh, R. (2015) Sensitive ELISA Method for the Measurement of
4 Catabolites of Antibody-Drug Conjugates (ADCs) in Target Cancer Cells. *Molecular*
5 *pharmaceutics* 12, 1752-61.
6
7 (25) Bissery, M. C., Guenard, D., Gueritte-Voegelein, F., and Lavelle, F. (1991) Experimental
8 antitumor activity of taxotere (RP 56976, NSC 628503), a taxol analogue. *Cancer Res* 51,
9 4845-52.
10
11 (26) Xie, H., Audette, C., Hoffee, M., Lambert, J. M., and Blattler, W. A. (2004)
12 Pharmacokinetics and biodistribution of the antitumor immunoconjugate, cantuzumab
13 mertansine (huC242-DM1), and its two components in mice. *The Journal of*
14 *pharmacology and experimental therapeutics* 308, 1073-82.
15
16 (27) Hong, E. E., Erickson, H., Lutz, R. J., Whiteman, K. R., Jones, G., Kovtun, Y., Blanc, V.,
17 and Lambert, J. M. (2015) Design of Coltuximab Ravtansine, a CD19-Targeting
18 Antibody-Drug Conjugate (ADC) for the Treatment of B-Cell Malignancies: Structure-
19 Activity Relationships and Preclinical Evaluation. *Molecular pharmaceutics* 12, 1703-16.
20
21 (28) Lin, D., Saleh, S., and Liebler, D. C. (2008) Reversibility of covalent electrophile-protein
22 adducts and chemical toxicity. *Chem Res Toxicol* 21, 2361-9.
23
24 (29) Baldwin, A. D., and Kiick, K. L. (2011) Tunable degradation of maleimide-thiol adducts
25 in reducing environments. *Bioconjug Chem* 22, 1946-53.
26
27 (30) Golfier, S., Kopitz, C., Kahnert, A., Heisler, I., Schatz, C. A., Stelte-Ludwig, B., Mayer-
28 Bartschmid, A., Unterschemmann, K., Bruder, S., Linden, L., et al. (2014) Anetumab
29 ravtansine: a novel mesothelin-targeting antibody-drug conjugate cures tumors with
30 heterogeneous target expression favored by bystander effect. *Mol Cancer Ther* 13, 1537-
31 48.
32
33 (31) Xia, T. S., Wang, J., Yin, H., Ding, Q., Zhang, Y. F., Yang, H. W., Liu, X. A., Dong, M.,
34 Du, Q., Ling, L. J., et al. (2010) Human tissue-specific microenvironment: an essential
35 requirement for mouse models of breast cancer. *Oncol Rep* 24, 203-11.
36
37 (32) Roussel, M. F., Downing, J. R., Rettenmier, C. W., and Sherr, C. J. (1988) A point
38 mutation in the extracellular domain of the human CSF-1 receptor (c-fms proto-oncogene
39 product) activates its transforming potential. *Cell* 55, 979-88.
40
41 (33) Bhargava, M., Joseph, A., Knesel, J., Halaban, R., Li, Y., Pang, S., Goldberg, I., Setter,
42 E., Donovan, M. A., Zarnegar, R., et al. (1992) Scatter factor and hepatocyte growth
43 factor: activities, properties, and mechanism. *Cell growth & differentiation : the*
44 *molecular biology journal of the American Association for Cancer Research* 3, 11-20.
45
46 (34) Yu, D. D., Wu, Y., Shen, H. Y., Lv, M. M., Chen, W. X., Zhang, X. H., Zhong, S. L.,
47 Tang, J. H., and Zhao, J. H. (2015) Exosomes in Development, Metastasis and Drug
48 Resistance of Breast Cancer. *Cancer science*.
49
50 (35) Fusek, M., Vetvickova, J., and Vetvicka, V. (2007) Secretion of cytokines in breast
51 cancer cells: the molecular mechanism of procathepsin D proliferative effects. *Journal of*
52 *interferon & cytokine research : the official journal of the International Society for*
53 *Interferon and Cytokine Research* 27, 191-9.
54
55
56
57
58
59
60

FIGURE FOR TOC (below)

